A KINETIC MECHANISM FOR ATMOSPHERIC PHOTOCHEMICAL REACTIONS

Appendix B

of

Development of a Simulation Model
for Estimating Ground Level Concentrations
of Photochemical Pollutants

Prepared by

Systems Applications, Inc.
Beverly Hills, California 90212

for the

Air Pollution Control Office
of the Environmental Protection Agency
Durham, North Carolina 27701

A KINETIC MECHANISM FOR ATMOSPHERIC PHOTOCHEMICAL REACTIONS

Appendix B

of

Development of a Simulation Model
for Estimating Ground Level Concentrations
of Photochemical Pollutants

John H. Seinfeld
Thomas A. Hecht
Philip M. Roth

Report 71SAI-9

May 1971

Prepared by

Systems Applications, Inc.
Beverly Hills, California 90212

for the

Air Pollution Control Office
of the Environmental Protection Agency
Durham, North Carolina 27701

under Contract CPA 70-148

CONTENTS

INTRODUCTION

The quantitative description of the rates of chemical reaction of atmospheric contaminants is a vital ingredient in the formulation of a model capable of predicting accurately ground level concentrations of gaseous pollutants. That this is true is evident from an inspection of the governing equations of the model, the equations of continuity:

$$\frac{\partial c_i}{\partial t} + v_x \frac{\partial c_i}{\partial x} + v_y \frac{\partial c_i}{\partial y} + v_z \frac{\partial c_i}{\partial z} = \frac{\partial}{\partial x}\left(K_x \frac{\partial c_i}{\partial x}\right) + \frac{\partial}{\partial y}\left(K_y \frac{\partial c_i}{\partial y}\right) + \frac{\partial}{\partial z}\left(K_z \frac{\partial c_i}{\partial z}\right)$$

$$+ R_i(c_1, c_2, \ldots, c_p) + S_i \qquad \text{(B-1)}$$

$$i = 1, 2, \ldots, p$$

where x, y = horizontal coordinates
z = vertical coordinate
v_x, v_y, v_z = three components of average wind velocity vector
c_i = time-smoothed concentration of species i
K_x, K_y, K_z = turbulent eddy diffusivities
S_i = rate of emission of species i from elevated sources,

a repetition of equations (2) in the main text. The reaction rate term, R_i, represents the rate of production of species i and is commonly expressed as the algebraic sum of the rates of production of species i over all chemical reactions in which species i participates. Thus,

$$R_i = \sum_{j=1}^{n} a_{ij} r_j = \sum_{j=1}^{n} a_{ij} k_j c_{j1} c_{j2}$$

where a_{ij} = -1 if species i is a reactant in reaction j, +1 if a product, 0 if not present.
and c_{j1}, c_{j2} = reactant concentrations in reaction j, assumed to involve two species ($c_{j2} = 1$ if reaction j involves one species).

Not only does $R_i(c_1, c_2, \ldots, c_p)$ appear in each of the partial differential equations that comprise the equations of continuity, but the common argument of all R_i, $i = 1, 2, \ldots, p$, links (or couples) these equations in such a way that their solution must be simultaneous. Thus, the successful development of a comprehensive airshed model depends heavily on the accuracy of description of reaction rate processes.

The formulation of a kinetic mechanism of general validity is an endeavor beset by several inherent difficulties. First, there is a multiplicity of stable chemical species present in the atmosphere. Most of these exist at very low concentrations, thereby creating major problems in detection and analysis. A number of atmospheric constituents, in fact, remain unidentified. Second, the large variety of highly reactive, short-lived intermediate species and free radicals further complicates the picture. Finally, when we consider the enormous number of individual chemical reactions that these species undergo, the barrier to understanding becomes clear. However, while we must admit

to only a limited knowledge of atmospheric reaction processes, it remains essential that we attempt to formulate quantitative descriptions of these processes which are suitable for inclusion in an overall simulation model.

The formulation and development of a kinetic mechanism that is to be incorporated in any airshed model is both delicate and exacting, an undertaking requiring a blend of science, craftsmanship, and art. Such a mechanism must not be overly complex, as computation times for integration of the continuity equations in which the mechanism is to be imbedded are likely to be excessive. On the other hand, too simplified a mechanism may omit important reaction steps, and thus be inadequate to describe atmospheric reaction processes. A major issue in this regard is the requirement that the mechanism predict the chemical behavior of a complex mixture of many hydrocarbons, yet do so with a paucity of detail.* Thus, the formulator must strike a careful balance in postulating a mechanism--between compactness of form and accuracy in prediction.

The kinetic mechanism, once developed, must be validated. This procedure is commonly conceived as consisting of two parts: validation in the absence of transport processes and validation in their presence. In practical terms we are speaking, respectively, of comparison of the model's predictions with data collected in smog chamber experiments and with data collected at actual contaminant monitoring stations situated in an urban airshed. When we speak of validation of a kinetic mechanism in this section, we are referring to the comparison between predictions and experiment based on smog chamber studies. The second and more complex of the two parts, validation of the kinetic mechanism in the presence of transport processes (convection and turbulent diffusion) is the primary undertaking of this project and is described in the main text.

Only the most intrepid of readers can have been exposed to the warnings and qualifications that highlight this discussion, and have emerged with faith undiminished. Yet one final caveat is necessary. Smog chamber experiments may be considered valid simulations of the atmosphere only under the following conditions: (1) wall effects are eliminated or are negligible, (2) contaminant concentrations are at levels found in the atmosphere, (3) the initial charge to the chamber is representative of urban source effluents and (4) the spectral distribution of the radiation is the same as that found in the atmosphere. It is unlikely that many smog chamber studies satisfy all these requirements.

As a part of the current contract effort, we undertook to identify an existing kinetic mechanism, or, if necessary, to develop a new mechanism, capable of meeting the following requirements for inclusion in an atmospheric simulation: relative simplicity, sufficient generality to include all major gaseous contaminant species (aerosols were not considered in the present study) and acceptable accuracy in the prediction of smog chamber data over

*Most mechanisms have been developed to simulate the photo-oxidation of a single hydrocarbon species, even though the model may include a general hydrocarbon as a reactant. It is important to note that the behavior of a mixture may be very different from the average behavior of unmixed hydrocarbons.

a range of values of NO_x/HC and for a variety of hydrocarbons. In Section I of this Appendix, we present an assessment of existing mechanisms, arriving at the conclusion that a "better" model was needed. Included are the results of the validation study for one of the more promising existing mechanisms and a discussion of the deficiencies of this and other formulations. In Section II, we present a new kinetic mechanism, one developed by Thomas A. Hecht and John H. Seinfeld of the California Institute of Technology. The results of recent validation studies, which are detailed in Section V, demonstrate that this model is capable of predicting with acceptable accuracy the concentration/time behavior of smog chamber experiments for propylene, isobutylene, n-butane, and a mixture of propylene and n-butane at initial NO_x to hydrocarbon ratios of 1/3 to 1. The mechanism has also been shown to simulate accurately the effect on photo-oxidation rates of variations in CO concentrations, as well as the inhibitory effect of high initial concentrations of nitric oxide on the maximum concentration of ozone obtained. Finally, in Section VI, we discuss the adaptation of this validated mechanism for use in an urban airshed model.

I. SURVEY OF PREVIOUSLY PROPOSED MECHANISMS

It is only in the last ten years that investigators have postulated general kinetic mechanisms to describe the rates of chemical reactions in the atmosphere.* The mechanisms that have been proposed can be classified as follows:

Class 1. Highly simplified mechanisms (fewer than ten reaction steps)

Friedlander and Seinfeld (1969)	general**
Eschenroeder (1969)	general
Behar (1970)	general

Class 2. Simplified mechanisms (ten to twenty-five reaction steps)

Wayne and Earnest (1969)	propylene
Behar (1970)	propylene

Class 3. Complex mechanisms (more than twenty-five reaction steps)

Westberg and Cohen (1969)	isobutylene
Wayne, et al. (1970)	general

(There are, in addition, several mechanisms under development or recently completed that have not been reported. These include a Class 2 mechanism of Eschenroeder and Class 2 and 3 mechanisms of Hecht and Seinfeld. As we have adopted the Class 2 mechanism of Hecht and Seinfeld for use in the development of our airshed model, we discuss this mechanism in Section II of this Appendix.)

---

* This is in contrast to the very considerable efforts that have been expended by scores of investigators over the past two decades in the study of individual atmospheric reactions. Since the literature in this field is voluminous, the interested reader is referred initially to reviews and articles. Particularly recommended are the reviews by Leighton (1961), Altshuller and Bufalini (1965, 1971), and Johnston, et al. (1970).

**Refers to the hydrocarbon species for which the mechanism was developed.

At the outset of this project, we were faced with the choice of adopting an existing mechanism or developing a new mechanism. What follows is a synopsis of the arguments leading to our eventual decision--the development of a new mechanism.

- Class 3 mechanisms were ruled out for three reasons. First, while the aim of those developed thus far has been completeness of description, this thoroughness has been achieved through the inclusion of a number of reaction steps that involve free radicals. Unfortunately, knowledge of the rates of these reactions is imprecise. Furthermore, when several free radical reactions are included in a mechanism, the flexibility in the choice of rate constants is increased, as each imprecisely known parameter can be varied independently in the process of matching prediction and experiment. To the extent that Class 3 mechanisms possess this flexibility in parameterization, the validity of comparison of prediction and experiment is diminished.*

  Second, computation time is a limiting factor in the solution of the coupled partial differential equations that comprise the overall airshed model. The inclusion of a Class 3 mechanism in such a model greatly increases the computational burden and is to be avoided if at all possible.

  Finally, the decision to develop and implement a Class 3 mechanism implies the desire to represent reaction processes as accurately as is feasible. Thus, a relatively large number of reaction steps must be incorporated in a description of the dynamics of consumption of *a particular hydrocarbon*, such as propylene. Reaction dynamics will, however, vary for the many hydrocarbon species present in the atmosphere. If, for example, thirty to

---

*A statistical analogy is useful in illustrating this point. It is well known that the sum of a linear combination of n normally distributed, independent random variables is also normally distributed, with variance equal to n times the variance of each individual variable (assumed equal).

Thus, if $\eta = \sum_{i=1}^{n} a_i x_i$, $V(\eta) = \sum_{i=1}^{n} x_i^2 \, V(a_i)$. Further, if $V(a_1) = \ldots = V(a_n)$,

$V(\eta) = nV(a_1) \sum_{i=1}^{n} x_i^2$. Finally, if $x_1 = x_2 = \ldots = x_n = 1$, $V(\eta) = nV(a_1)$.

Hence, the variance of the predicted value η (or the uncertainty associated with prediction) is proportional to n, the number of terms in the original equation.

Consider now that the reaction rate constants, k_i, have associated with them a measure of uncertainty, $V(k_i)$. We can now argue, in an analogous manner, that the greater the number of reaction steps that are included in a mechanism, the larger will be the uncertainty associated with the prediction of concentration, which is a complex function of the k_i, $i = 1, 2, \ldots, n$. Thus, parsimony in parameterization is a desirable attribute in a kinetic mechanism.

forty steps are required to describe propylene kinetics, and fifty hydrocarbon species, each having unique dynamics, are believed to exert a significant impact on atmospheric reaction processes, one is faced with an intractable representation of the system. Alternatively, adoption of a detailed representation of the reactions of a single species (for example, propylene) which may, upon development, be applied to a single, generalized hydrocarbon is tantamount to constructing a mechanism having many of the representational deficiencies of a Class 1 or Class 2 kinetic scheme and, in addition, introduces a substantial parameter estimation problem. For these reasons, we turned to Class 1 and Class 2 mechanisms.

- We had hoped, for obvious reasons of simplicity and convenience, that it would be possible to employ a Class 1 mechanism in the overall airshed model. We thus undertook a validation study for one of the three Class 1 mechanisms cited, that of Eschenroeder (1969). (It is unnecessary to study the Class 1 mechanisms of Friedlander and Seinfeld and of Behar, as it can be shown that Eschenroeder's mechanism, slightly modified*, is substantially the same as, or superior to, the other two (see Table B-1 for details of this mechanism.)**

  Five computer runs were carried out to test the accuracy of prediction of the modified mechanism when compared with smog chamber studies for propylene.

Run	Data Source	Propylene/NO	Rate Constants***	Figure
1	Gulf Research CRC-3	1.93	Original	B-1
2	Gulf Research CRC-3	1.93	Revised	B-2
3	Gulf Research CRC-311	5.35	Original	B-3
4	Gulf Research CRC-311	5.35	Revised	B-4
5	California State Air Resources Board	0.91	Original	B-5

  Calculated values and experimental data for the five runs are plotted in Figures B-1 to B-5 respectively. While the results shown in Figure B-2, employing revised rate constants, demonstrated a distinct improvement over the results of Figure B-1, based on Eschenroeder's original published constants, these revised constants did not bring about a similar improvement in accuracy of prediction for a Gulf data CRC-311 (see Figures B-3 and B-4). Also, the mechanism was unable to predict NO_2 and O_3 concentration behavior

---

*The reaction $RO_2^{\cdot} + O_2 \rightarrow RO^{\cdot} + cO_3$ was eliminated because of its endothermicity.

**The Friedlander and Seinfeld and the modified Eschenroeder mechanisms differ in that the assumption of pseudo-steady state (or quasi-equilibrium) is invoked for ozone in the former. The Behar and Eschenroeder mechanisms are at variance only in the choice of stoichiometric coefficients.

***See Table B-2 for a summary of original and revised reaction rate constants.

Figures B-1 to B-5 and Tables B-1 and B-2 follow

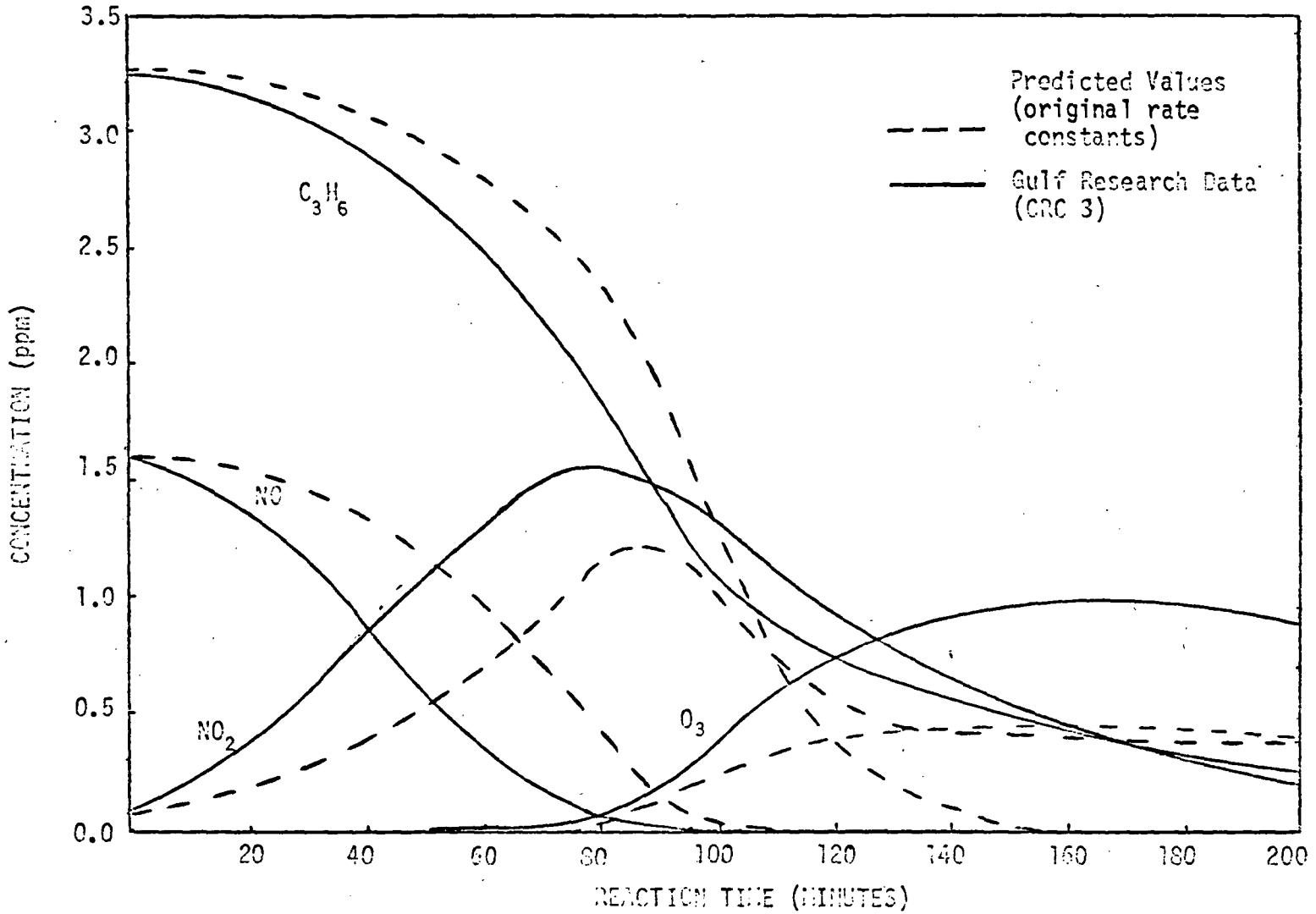

FIGURE B-1. VALIDATION OF THE MODIFIED ESCHENROEDER MECHANISM - RUN 1

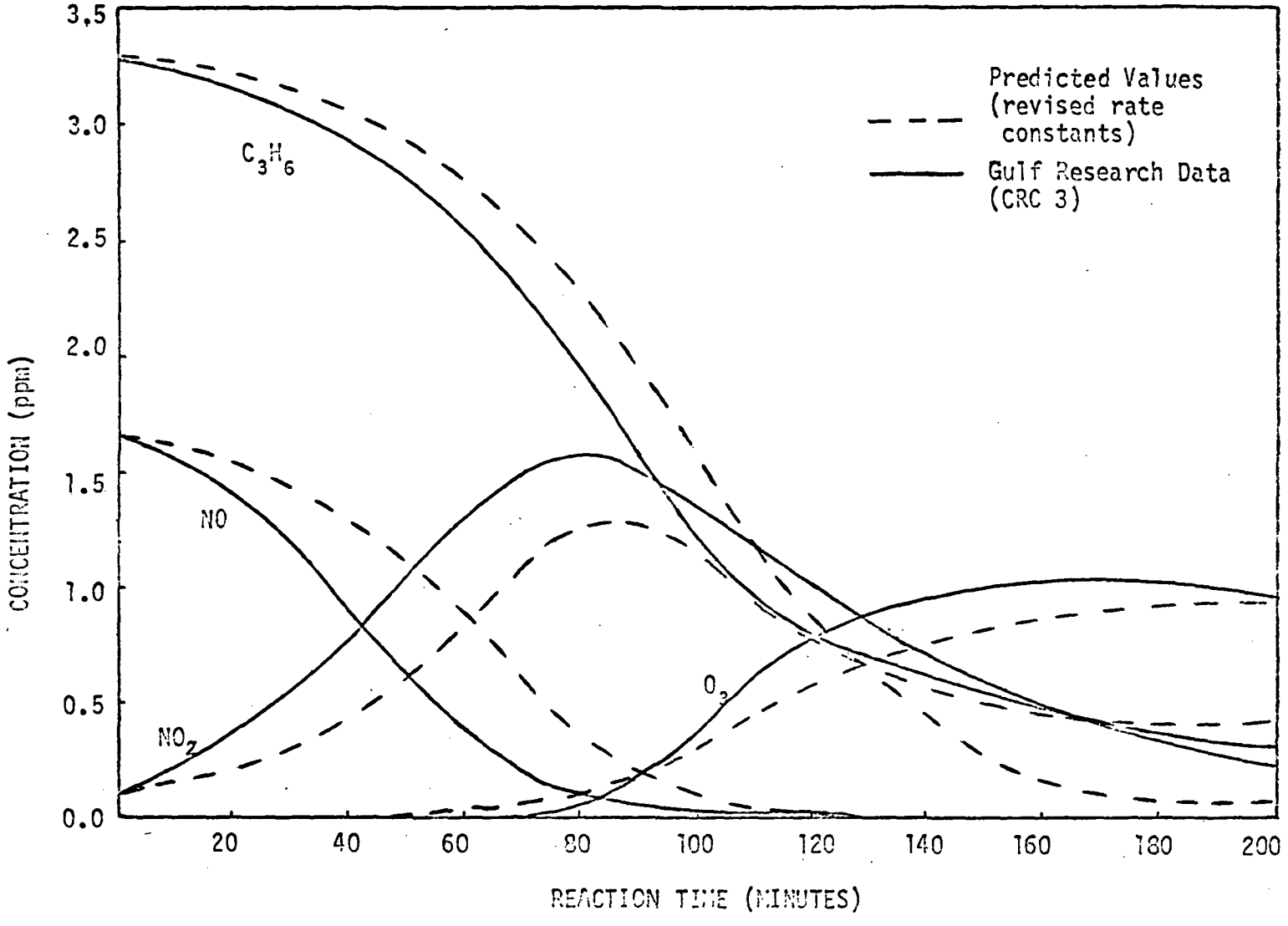

FIGURE B-2. VALIDATION OF THE MODIFIED ESCHENROEDER MECHANISM - RUN 2

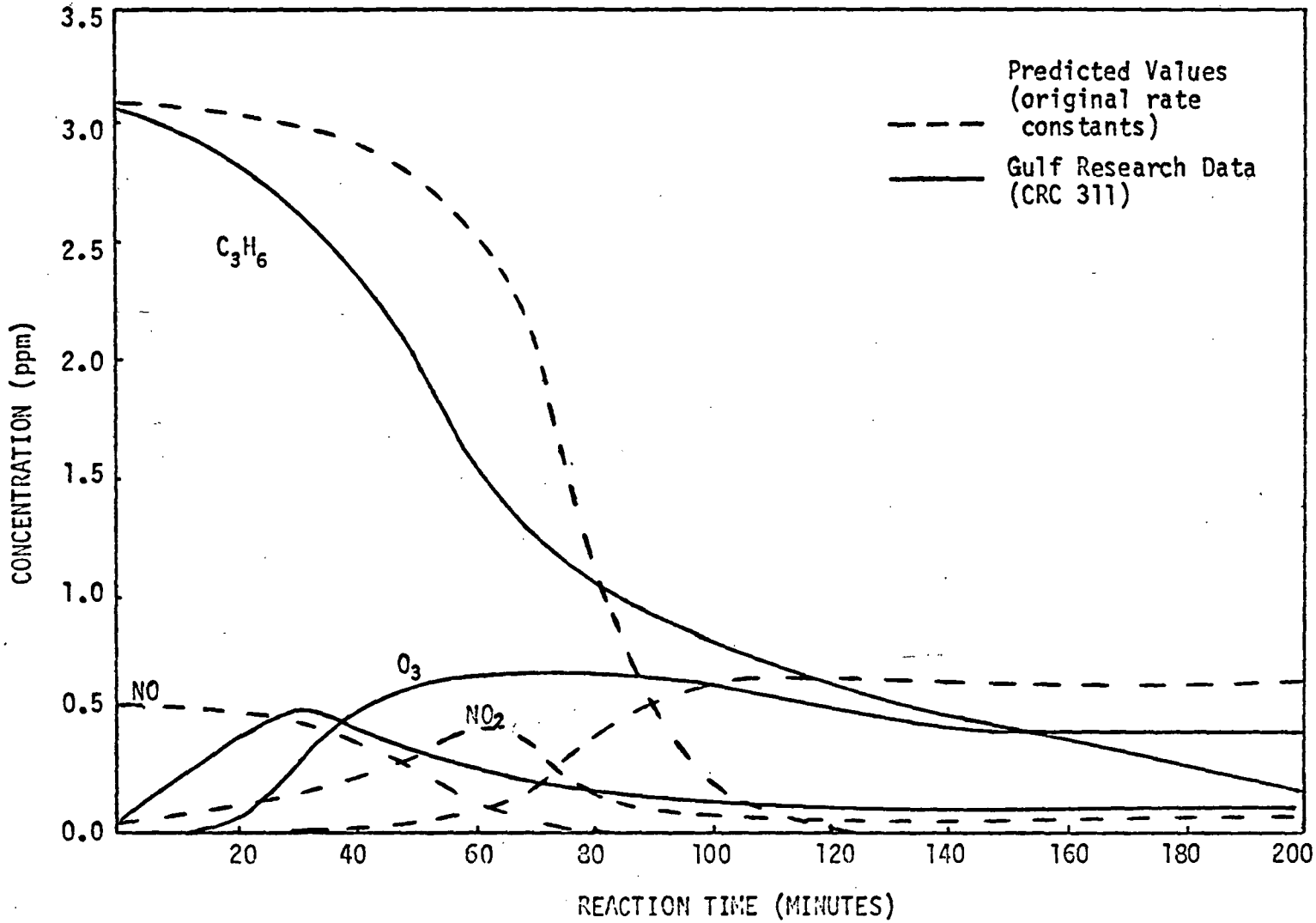

FIGURE B-3. VALIDATION OF THE MODIFIED ESCHENROEDER MECHANISM - RUN 3

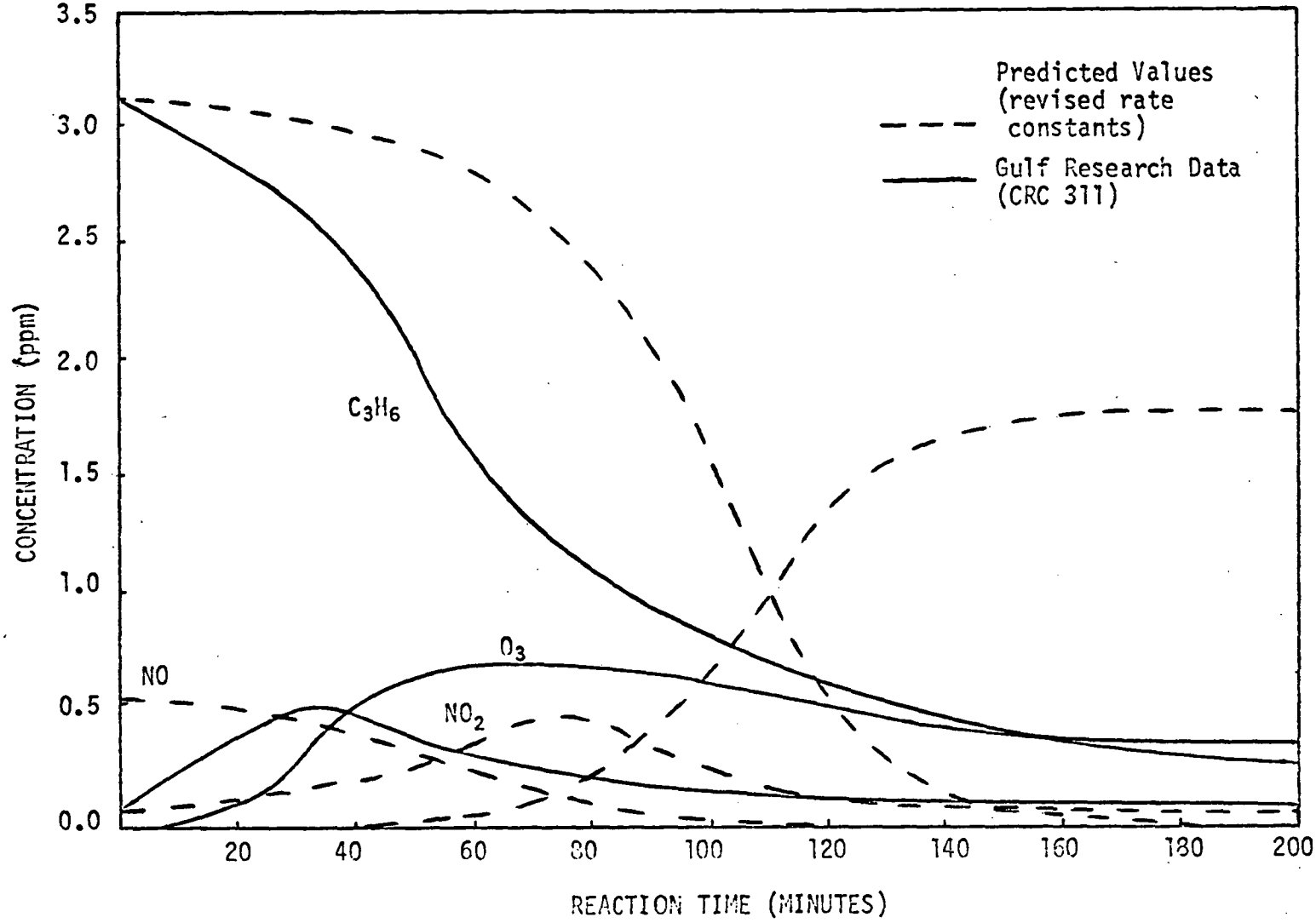

FIGURE B-4. VALIDATION OF THE MODIFIED ESCHENROEDER MECHANISM - RUN 4

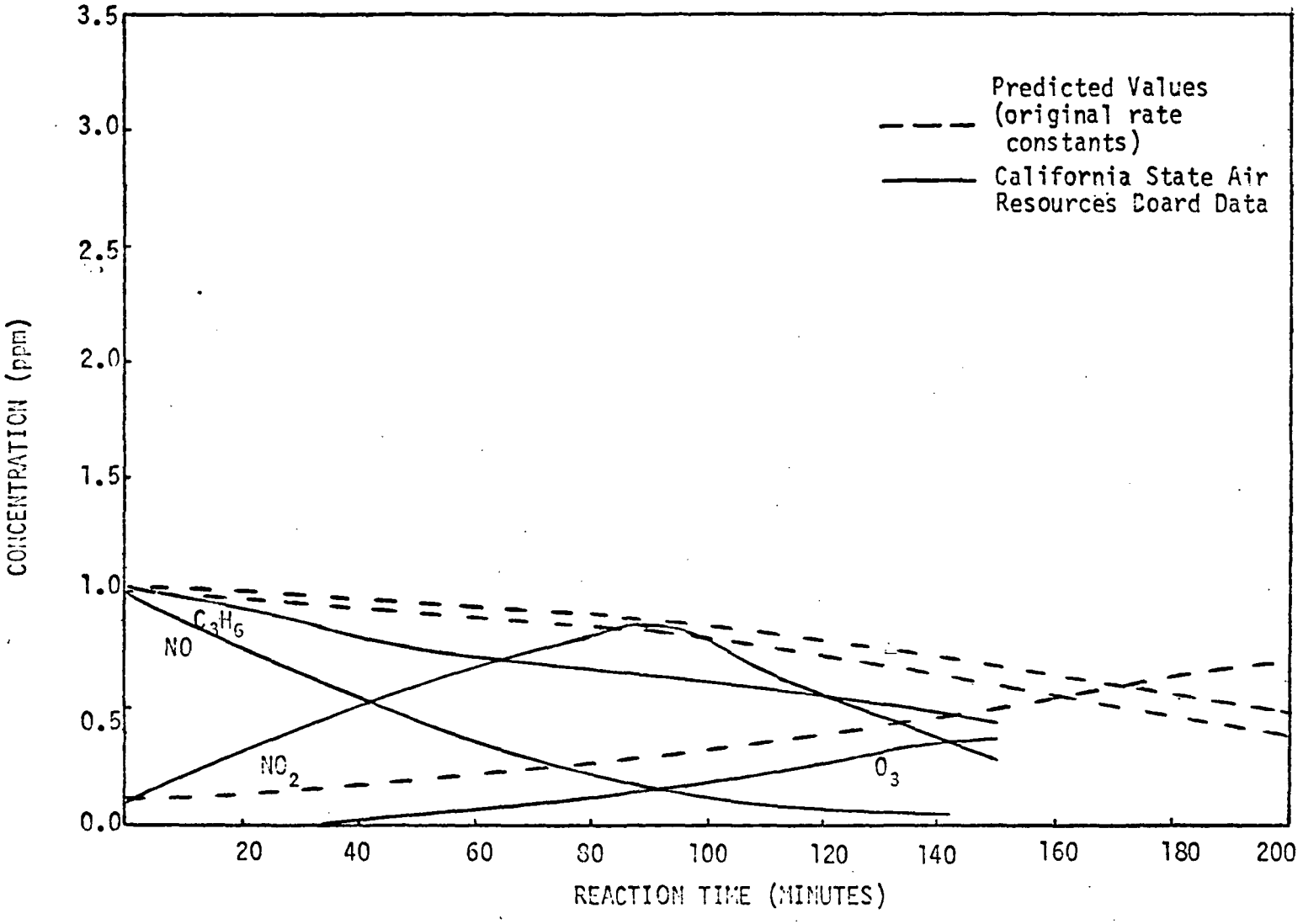

FIGURE 3-5. VALIDATION OF THE MODIFIED ESCHENROEDER MECHANISM - RUN 5

TABLE B-1. The Modified Class 1

Mechanism of Eschenroeder (1969)

$$NO_2 + h\nu \xrightarrow{1} NO + O$$

$$O + O_2 + M \xrightarrow{2} O_3 + M$$

$$O_3 + NO \xrightarrow{3} NO_2 + O_2$$

$$HC + O \xrightarrow{4} bRO_2^{\bullet} + cRCHO$$

$$HC + O_3 \xrightarrow{5} bRO_2^{\bullet} + cRCHO$$

$$RO_2^{\bullet} + NO \xrightarrow{6} NO_2 + RO\bullet$$

$$RO_2^{\bullet} + O_2 \xrightarrow{7} dO_3 + RO\bullet$$

$$RO_2^{\bullet} + NO_2 \xrightarrow{8} aPAN$$

Steady state assumed for atomic oxygen and $RO_2^{\bullet}$.

TABLE B-2. Reaction Rate Constants and Stoichiometric Coefficients for the Modified Eschenroeder Mechanism (Propylene)

i (units)	k_i	
	Original*	Revised
1 (min^{-1})	0.40	0.37
2 (min^{-1})	2.76×10^6	2.0×10^6
3 ($ppm^{-1}\ min^{-1}$)	21.8	21.8
4 ($ppm^{-1}\ min^{-1}$)	4.97×10^4	4.97×10^4
5 ($ppm^{-1}\ min^{-1}$)	.18	0.05
6 ($ppm^{-1}\ min^{-1}$)	50.0	50.0
7 (min^{-1})	6.285	6.285
8 ($ppm^{-1}\ min^{-1}$)	3.0	3.0
Stoichiometric Coefficients		
b	2.5	2.5
d	0.5	0.7

*Eschenroeder (1969)

for the Air Resources Board data (see Figure B-5). We therefore dismissed the possibility of employing this mechanism, and thus all available Class 1 mechanisms, in the overall airshed model.

- The two Class 2 mechanisms that have been postulated, those of Wayne and Earnest (1969) and Behar (1970), were found to be unsatisfactory for two reasons. First, both mechanisms omit certain reaction steps which are now thought to be significant (as, of course, do the simpler Class 1 mechanisms) and which have been incorporated into the newly developed model discussed in Section II. These steps are the formation of nitric acid, the formation of nitrous acid and its photolysis to form OH· radicals, the acceleration of NO_2 and O_3 formation (due indirectly to the reaction of CO with the OH· radical), and the oxidation of hydrocarbon species by OH· radicals. Second, both models include reaction steps, primarily involving free radicals, about which little is known. This situation is similar to that described earlier in the discussion of Class 3 mechanisms, in which a model can be manipulated to fit what data exist.

These, then, are the arguments that led to the development of a new mechanism, which is described in the following section.

II. A NEW SIMPLIFIED MECHANISM

Let us first briefly review the necessary attributes of a kinetic mechanism that is to be a part of an urban airshed model. A suitable mechanism must: (1) describe reaction rate phenomena accurately over a specified range of concentrations, (2) be a parsimonious representation of the actual atmospheric chemistry, in the interest of minimizing computation time, and (3) be written for a general hydrocarbon species, with the inclusion of variable stoichiometric coefficients to permit simulation of the behavior of the complex hydrocarbon mixture that actually exists in the atmosphere. In short, an acceptable mechanism must exhibit a balance between accuracy of prediction and ease of computation. We present in this section a new, simplified (or Class 2) mechanism for describing the rates of atmospheric chemical reactions that we believe satisfies these requirements.

At this point we direct the reader to Table B-3 for a complete statement of the new mechanism; reference should be made to this table throughout the discussion that follows. Description of the mechanism is facilitated by splitting the presentation into three parts--a brief discussion of the reactions of inorganic species, a more detailed discussion of hydrocarbon reactions, and a presentation of the mathematical equations associated with the mechanism.

A. Inorganic reactions

The major inorganic species that participate in atmospheric chemical reactions are NO, NO_2, O_2, O_3, CO, and H_2O. The reactions

Table B-3 follows

Table B-3. The New, Simplified Mechanism

$$NO_2 + h\nu \xrightarrow{1} NO + O$$

$$O + O_2 + M \xrightarrow{2} O_3 + M$$

$$O_3 + NO \xrightarrow{3} NO_2 + O_2$$

$$O_3 + 2NO_2 \xrightarrow[H_2O]{4} 2HNO_3 \ *$$

$$NO + NO_2 \xrightarrow[H_2O]{5} 2HNO_2$$

$$HNO_2 + h\nu \xrightarrow{6} OH\cdot + NO$$

$$CO + OH\cdot \xrightarrow[O_2]{7} CO_2 + HO_2\cdot$$

$$HO_2\cdot + NO_2 \xrightarrow{8} HNO_2 + O_2$$

$$HC + O \xrightarrow{9} \alpha RO_2\cdot$$

$$HC + O_3 \xrightarrow{10} \beta RO_2\cdot + \gamma RCHO$$

$$HC + OH\cdot \xrightarrow{11} \delta RO_2\cdot + \varepsilon RCHO$$

$$RO_2\cdot + NO \xrightarrow{12} NO_2 + \theta OH\cdot$$

$$RO_2\cdot + NO_2 \xrightarrow{13} PAN$$

$$HO_2\cdot + NO \xrightarrow{14} NO_2 + OH\cdot$$

---

*Reaction 4 is a composite of the three reactions,

$$O_3 + NO_2 \xrightarrow{4a} NO_3 + O_2$$

$$NO_3 + NO_2 \xrightarrow{4b} N_2O_5$$

$$N_2O_5 + H_2O \xrightarrow{4c} 2HNO_3$$

Thus, it is not necessary to retain NO_3 in the mechanism.

of these five species are represented by reactions 1 through 8 and reaction 14 in Table B-3. In particular, these nine reactions account for the following experimentally observed phenomena:

1. the primary inorganic reactions in the formation of photochemical pollutants (reactions 1 to 3)

2. formation of nitric acid (reaction 4)

3. formation and photolysis of nitrous acid (reactions 5, 6 and 8)

4. the reaction of CO and OH· radicals (reaction 7)

Reactions 5 and 6 have been included to account for the importance of HNO_2 as a source of OH· radicals in the presence of water. In a dry system, reactions 4 and 5 will be omitted. Reaction 8 is included to provide for the consumption of HO_2· when NO has been depleted. The importance of these phenomena has been demonstrated in recent smog chamber experiments reported by Stedman, et al. (1970), Holmes (1970), and Westberg, et al. (1971).

B. Organic reactions

In the development of a simplified mechanism, it is helpful to introduce a general hydrocarbon species, denoted HC, which may be taken to represent a single hydrocarbon or a mixture of hydrocarbons. In explaining the development of the mechanism, however, we classify individual hydrocarbons as belonging to one of three groups--olefins, aromatics, and paraffins. (The reactions of oxygenated hydrocarbons have been ignored). We can then consider the reactions of atomic oxygen (O), ozone (O_3), and the hydroxyl radical (OH·) with hydrocarbons belonging to each of the three groups.

The reaction of atomic oxygen with an olefin results in the production of two free radicals, generally an alkyl and an acyl. For example, the reaction of atomic oxygen with ethylene produces CH_3· + HĊO; with propylene, CH_3· + CH_3ĊO or C_2H_5· + HĊO; with isobutylene, $(CH_3)_2$ CH· + HCO or C_2H_5· + CH_3ĊO. These alkyl and acyl radicals, in turn, react rapidly with molecular oxygen to form peroxyalkyl and peroxyacyl radicals. The reactions of atomic oxygen with aromatics is in some cases also rapid (Leighton (1961, p. 146)). While peroxides, acids and alcohols have been observed as final products of the reaction chain initiated by the attack of atomic oxygen on aromatics (Eventova and Prytkova, (1960)); Kemula and Grabowska, (1960)), the initial products are not well known. The main reaction of atomic oxygen with paraffins is most probably RH + O$\longrightarrow$R· + OH· (Leighton (1961, p. 142)). This reaction is relatively slow, although the reaction rate increases significantly with molecular weight.

In summary, the main result of the reaction of atomic oxygen with hydrocarbons is the formation of free radicals, usually two in number. We represent this step in the mechanism as

$$HC + O \xrightarrow{9} \alpha RO_2\cdot$$

where $RO_2\cdot$ is a lumped radical species (in general, a peroxyalkyl or peroxyacyl radical) and α is the stoichiometric coefficient, i.e., the number of radicals produced in this reaction. It should be noted that $RO_2\cdot$ represents the total population of oxygen-containing free radicals which are capable of oxidizing NO to NO_2. However, $RO_2\cdot$ is merely symbolic of these radicals; some may not contain exactly two oxygen atoms (for example, peroxyacyl radicals).

We now consider the reactions of ozone with hydrocarbons. The initial products of the olefin ozone reaction are an aldehyde and a zwitterion. The number of free radicals formed depends on the subsequent zwitterion reaction. For three common olefins, the result of O attack is:

ethylene	$HCHO + CH_2O_2$
propylene	$HCHO + C_2H_4O_2$ or $CH_3CHO + CH_2O_2$
isobutylene	$HCHO + (CH_3)_2CO_2$ or $(CH_3)_2CO + CH_2O_2$

The reaction of ozone with alkanes and aromatics is slow and can probably be neglected. Thus, the initial reactions of hydrocarbon with ozone can be summarized as

$$HC + O_3 \xrightarrow{10} \beta RO_2\cdot + \gamma RCHO$$

where β and γ are stoichiometric coefficients whose values depend on the composition of the hydrocarbon mixture.

We now consider the reactions of $OH\cdot$ with various hydrocarbons. Hecht and Seinfeld (1971) have proposed three possible mechanisms for the propylene/$OH\cdot$ reaction. In the first two, aldehydes and free radicals are the products, and, in the third, the chain reaction is terminated by the formation of the allyl radical and water. The alkane/$OH\cdot$ reaction has been recently considered by Greiner (1970). He postulates that the principal products of this reaction are a free radical and water. We might also expect that the branched aromatic/$OH\cdot$ reaction would yield similar products. Taking into account each of these possible steps we include in the mechanism the general hydrocarbon/$OH\cdot$ reaction,

$$HC + OH\cdot \xrightarrow{11} \delta RO_2\cdot + \varepsilon RCHO$$

where the stoichiometric coefficients δ and ε are again a function of the particular hydrocarbon mixture. Since aldehyde formation occurs only through the reaction of olefins (and possibly aromatics), ε will be less than one.

The remaining organic reactions in the simplified mechanism describe the oxidation of NO to NO_2 by peroxy radicals and the formation of PAN.

$$RO_2\cdot + NO \xrightarrow{12} NO_2 + \theta OH\cdot$$

$$RO_2\cdot + NO_2 \xrightarrow{13} PAN$$

It is important to note that, if CO and H_2O are present, we treat $HO_2\cdot$ and $RO_2\cdot$ as separate species. In the absence of CO and H_2O, however, we consider only the single species $RO_2\cdot$, which must now include $HO_2\cdot$ since reactions 5-8 and reaction 14 are omitted. In this case, θ represents the fractional product of OH· from reaction 12, that is, the fraction of $HO_2\cdot$ in the total lumped radical species $RO_2\cdot$.

Certain classes of reactions have not been included in the postulated mechanism. For example, the formation of organic nitrates can be treated as a part of reaction 13 and thus has not been considered separately. Aldehyde decomposition is not included, but this may be accounted for through the adjustment of γ and ε. PAN decomposition and radical-radical recombination reactions have been neglected because of their relative unimportance. Most notable, however, is the complete omission of aerosols in this treatment.

C. A Mathematical Representation of the New Mechanism

The simplified mechanism consists of reactions 1 to 14 in Table B-3 and includes the following species: NO, NO_2, O_3, HC, O, OH·, $HO_2\cdot$, $RO_2\cdot$, HNO_2, HNO_3, RCHO, PAN. Differential equations are required for the first four species, steady state relations for the next five. The last three species are products and may also be represented by differential equations. In this section, we present the algebraic expressions for each of the fourteen reaction steps, the five steady state relationships, and the four coupled, first order, ordinary differential equations that constitute the mathematical representation of the reaction dynamics.

The individual reaction rate expressions may be written directly from Table B-3 and are;

$$r_1 = k_1(NO_2)$$

$$r_2 = [k_2(O_2)(M)](O) = k_2'(O)$$

$$r_3 = k_3(O_3)(NO)$$

$$r_4 = k_4(O_3)(NO_2)$$

$$r_5 = [k_5(H_2O)](NO)(NO_2) = k_5'(NO)(NO_2)$$

$$r_6 = k_6(HNO_2)$$

$$r_7 = [k_7(CO)(O_2)](OH\cdot) = k_7'(OH\cdot)$$

$$r_8 = k_8(HO_2\cdot)(NO_2)$$

$$r_9 = k_9(HC)(O)$$

$$r_{10} = k_{10}(HC)(O_3)$$

$$r_{11} = k_{11}(HC)(OH\cdot)$$

$$r_{12} = k_{12}(RO_2\cdot)(NO)$$

$$r_{13} = k_{13}(RO_2\cdot)(NO_2)$$

$$r_{14} = k_{14}(HO_2\cdot)(NO)$$

The constants k_2', k_5', and k_7' are each defined as the product of the individual rate constant and concentration of a species present in sufficiently large concentrations that k_2', k_5' and k_7' may be considered invariant.

Now applying the steady state assumption to the species O, OH·, $HO_2\cdot$, $RO_2\cdot$, and HNO_2, we have:

$$O: \quad r_1 - r_2 - r_9 = 0$$

$$HNO_2: \quad 2r_5 - r_6 + r_8 = 0$$

$$OH\cdot: \quad r_6 - r_7 - r_{11} + \theta r_{12} + r_{14} = 0$$

$$RO_2\cdot: \quad \alpha r_9 + \beta r_{10} + \delta r_{11} - r_{12} - r_{13} = 0$$

$$HO_2\cdot: \quad r_7 - r_8 - r_{14} = 0$$

Substituting the individual reaction rate expressions into these five equations, we have:

$$(O) = \frac{k_1(NO_2)}{k_2' + k_9(HC)}$$

$$(OH\cdot) = \left[2k_5'(NO)(NO_2)\{k_{12}(NO) + k_{13}(NO_2)\} + \theta k_{12}(NO)\{\alpha k_9(HC)(O) + \beta k_{10}(HC)(O_3)\}\right]/B$$

$$(HO_2\cdot) = \frac{k_7'(OH\cdot)}{k_8(NO_2) + k_{14}(NO)}$$

$$(HNO_2) = \frac{k_8(HO_2\cdot)(NO_2) + 2k_5'(NO)(NO_2)}{k_6}$$

$$(RO_2\cdot) = \left[k_{11}(HC)\{\alpha k_9(HC)(O) + \beta k_{10}(HC)(O_3)\} + 2\delta k_5' k_{11}(HC)(NO)(NO_1)\right]/B$$

where $B = k_{11}(HC)\{k_{12}(NO) + k_{13}(NO_2)\} - \delta\theta k_{11}k_{12}(NO)(HC)$

The differential equations expressing the rate of formation of HC, NO, NO_2, and O_3 can be written directly from the reaction steps shown in Table B-3.

$$\frac{d(HC)}{dt} = -r_9 - r_{10} - r_{11} \qquad \text{(B-2a)}$$

$$\frac{d(NO)}{dt} = r_1 - r_3 - r_5 + r_6 - r_{12} - r_{14} \qquad \text{(B-2b)}$$

$$\frac{d(NO_2)}{dt} = -r_1 + r_3 - 2r_4 - r_5 - r_8 + r_{12} - r_{13} + r_{14} \qquad \text{(B-2c)}$$

$$\frac{d(O_3)}{dt} = r_2 - r_3 - r_4 - r_{10} \qquad \text{(B-2d)}$$

By substituting into these four differential equations the fourteen individual reaction rate expressions, we have a set of equations that is a function of the concentrations of the four species, HC, NO, NO_2, and O_3, and also a function of the steady state concentrations of O, HNO_2, $OH\cdot$, $RO_2\cdot$, and $HO_2\cdot$. Given initial concentrations of NO, NO_2, CO, O_3 and HC, these four differential equations may be integrated numerically (see Section IV) to predict the concentration/time behavior of the four components for which the equations are written. Note, however, that at each time step it is necessary to calculate new steady state concentrations of O, HNO_2, $OH\cdot$, $RO_2\cdot$, and $HO_2\cdot$ as a function of the most recent values of NO, NO_2, O_3 and HC.

Finally, if we wish to compute the concentration of products as a function of time, we add three differential equations to the original set of four:

$$\frac{d(RCHO)}{dt} = r_{10} + \varepsilon r_{11}$$

$$\frac{d(HNO_3)}{dt} = 2r_4$$

$$\frac{d(PAN)}{dt} = r_{13}$$

where (PAN) indicates all of the organic nitrate termination products of reaction 13.

III. PARAMETERS OF THE NEW MECHANISM

Prior to validation, it is necessary to establish values for the two classes of parameters that appear in the mathematical statement of the new kinetic mechanism--the reaction rate constants and the stoichiometric coefficients. For the most part, values of the rate constants can be estimated from the chemical literature. However, the values of certain rate constants, particularly those associated with the reactions of the generalized species, HC and $RO_2\cdot$, must be deduced from data available for individual species. Furthermore, there is a sacrifice of chemical detail inherent in the adoption of generalized species, a loss in the ability to associate the rate constant values with particular reactions. Thus, the rate constants in the simplified mechanism are more

a quantitative assessment of the relative rates of competing reactions than a reflection of the exact values for particular reactions. Similar difficulties are encountered in establishing values for the generalized stoichiometric coefficients that are included in the mechanism, as it is not possible to write a balanced reaction expression for a lumped hydrocarbon species.

In general, "base" values of rate constants that appear in the kinetic mechanism will be derived from published values. It should be kept in mind, however, that final values, established during validation of the mechanism, will in some cases differ from these base values. The rationale for selection of final values of parameters is presented in Section V. In this section we present the arguments for assigning base values to both the rate constants and the stoichiometric coefficients of the mechanism.

A. Reaction Rate Constants

We present in this section the base values of the reaction rate constants of the new mechanism. These values are summarized in Tables B-4 and B-5. The rate constants, k_1 and k_6, which depend on irradiation conditions, are treated separately in part A of Section VI.

The selection of certain rate constants requires some comment. Reaction 4 is a composite of three reactions:

$$O_3 + NO_2 \xrightarrow{4a} NO_3 + O_2$$

$$NO_3 + NO_2 \xrightarrow{4b} N_2O_5$$

$$N_2O_5 + H_2O \xrightarrow{4c} 2HNO_3$$

Reaction 4a will be rate controlling, as NO_3 reacts rapidly with NO_2. Reaction 4c will also proceed rapidly in the presence of water at concentrations typically found in the atmosphere. However, if the concentration of water is low, this reaction may compete with 4a. We thus regard the base value of k_{4a} as an upper limit for k_4. Similarly, reaction 7 is a composite of two reactions:

$$CO + OH\cdot \xrightarrow{7a} CO_2 + H\cdot$$

$$H\cdot + O_2 \xrightarrow{7b} HO_2\cdot$$

In this case, however, we assume that 7b is instantaneous, so that the rate of reaction 7 may be taken as that of 7a.

The values of rate constants presented in Table B-5 are for the reactions of representative hydrocarbon species. Thus, they have not been adopted directly. Rate constants for reactions 12 and 13 are not generally available.

Tables B-4 and B-5 follow

TABLE B-4. Base Values of Reaction Rate Constants for the Inorganic Reactions Included in the Simplified Mechanism

Reaction	Units	Specific Value or Range of Values	Reference
2	min^{-1} (pseudo first order)	2.76×10^{6}	Kaufman, et al. (1967)
3	ppm^{-1} min^{-1}	21.8	Clyne, et al. (1964)
4a	ppm^{-1} min^{-1}	0.0485	Ford, et al. (1957)
4b	ppm^{-1} min^{-1}	5.41×10^{3}	Schott and Davidson (1958)
4c	ppm^{-1} min^{-1}	2.94×10^{-3}	Zafonte (1970)
5	ppm^{-2} min^{-1}	4.3×10^{-6}	Wayne and Yost (1951)
7a	ppm^{-1} min^{-1}	200	Baulch, et al. (1968)
8	ppm^{-1} min^{-1}	10	No reported values. Value given estimated by authors.
14	ppm^{-1} min^{-1}	2.94	Johnston, et al. (1970).

TABLE B-5. Reaction Rate Constants for Individual Organic Species*

Reaction	Species	Rate Constant (ppm^{-1} min^{-1})
9	ethylene	770
	propylene	6850
	n-butane	32
	acetaldehyde	545
10	ethylene	4×10^{-3}
	propylene	1.6×10^{-2}
	isobutylene	3.4×10^{-2}
	trans-2-butane	0.63
11	n-butane	5.7×10^{3}
	ethylene	7.5×10^{3}
	formaldehyde	150
	acetaldehyde	25

*Values taken from Zafonte (1970).

B. Generalized Stoichiometric Coefficients

Stoichiometric coefficients are those parameters introduced into each individual reaction step to satisfy the requirement of conservation of mass. For example, in the reaction $NO_3 + NO_2 + H_2O \xrightarrow{5} 2HNO_3$, the "2" preceding HNO_3 is a stoichiometric coefficient. While these coefficients, in general, are easily established by carrying out a mass balance for all elements appearing in the reaction expression, a problem arises in the treatment of vaguely defined species such as the generalized hydrocarbon, HC. We cannot specify the exact number of atoms that comprise this fictitious species, and thus it is impossible to derive or compute appropriate coefficients. To skirt this problem, we introduce flexible parameters, termed "generalized" stoichiometric coefficients, such as α in the reaction, $HC + O \xrightarrow{9} \alpha RO_2$. These generalized coefficients must be established through deductive procedures such as "chemical" arguments and trial and error calculations. In the discussion that follows, we present the rationale for selecting the generalized coefficients, α, β, γ, δ, ε, and θ, introduced in the new mechanism.

We first consider the selection of a value for α, the number of radicals formed in the reaction of hydrocarbon and atomic oxygen. This choice is of prime importance, as α strongly governs the chain length of the reaction*, and the hydrocarbon/atomic oxygen reaction itself is critical in determining the rate of oxidation of NO to NO_2. Extensive validation studies have shown that in some cases α is most realistically treated as a function of the NO:HC ratio over the course of the reaction, rather than as a constant. Since α governs the chain length, this parameter should reflect the inhibitory effect of large NO:HC ratios on the formation of ozone. It was therefore decided that the instantaneous value of a α should depend on the NO:HC ratio as it changes with time. We would expect the values of α to lie between 2 and 10, depending on the particular hydrocarbon mixture and the NO:HC ratio.

The stoichiometric coefficient β, represents the number of oxygen-containing radicals produced as a result of the reaction of hydrocarbons with ozone. This coefficient is approximately two for olefins and somewhat less for mixtures of olefins and paraffins. We have treated β as a constant, as it is not necessary that both α and β vary with NO:HC ratio. Thus β is less than two and is a function of the composition of the hydrocarbon mixture.

The stoichiometric coefficient δ in reaction 11 is analogous to α and β, in that it governs the number of $RO_2\cdot$ radicals formed due to reaction of hydrocarbons--in this instance, with hydroxyl radicals. As in the case of β and for similar reasons, we have chosen to keep δ constant. The basic values of δ are not as tightly constrained, and thus less certain than those of β, because less is known about

*Chain length is defined as the average number of free radical reactions (or propagation steps) that occur as a result of each initiation reaction.

hydrocarbon/hydroxyl radical reactions than about hydrocarbon/ozone reactions. We expect, however, that δ will be about one, since likely products of the HC/OH· reaction are one free radical and an aldehyde (in the case of olefins) or water (in the case of paraffins).

The coefficients γ and ε determine the amount of aldehyde formed as a result of reactions 10 and 11. Neither of these coefficients should exceed one, with reasonable values lying between 0.5 and 1.0. In the validation studies to be described we did not compute aldehyde concentrations; thus the specification of γ and ε was not necessary.

The generalized coefficients δ (for RO_2· in the HC/OH· reaction) and θ (for OH· in the RO_2·/NO reaction) are important in simulating the effect of CO. Since OH· attacks both HC and CO and since the products of both reactions are radical species capable of oxidizing NO to NO_2 (RO_2· in the former case and HO_2· in the latter), it is necessary that the number of HO_2· radicals formed in the CO/OH· reaction (always equal to one) be greater than the number of RO_2· radicals formed in the HC/OH· reaction in the presence of CO. If the product $\delta\theta$ were greater than one, CO would effectively inhibit the rate of NO oxidization. This effect would be attributable to the scavenging of OH· radicals by CO, thereby diminishing the supply of OH· available for possible reaction with HC, a reaction capable of generating more radicals than the single HO_2· produced in the CO/OH· reaction. This point can also be verified by inspection of equation B-2h. If $\delta\theta > 1$, the negative terms $(1-\delta\theta)$ in the denominator become positive, d(NO)/dt is then also positive, and NO is not converted to NO_2. Thus, we require that $\delta\theta < 1$. Finally, the value of θ must be less than one, as all RO_2· are actually HO_2· if θ is equal to one. Unfortunately, there is little more that can be said about this coefficient.

IV. NUMERICAL INTEGRATION OF THE REACTION RATE EQUATIONS

In general, the rate equations for a system of chemical reactions among n species can be written in the form

$$\frac{dc_i}{dt} = f_i\ (c_1, \ldots, c_n) \qquad i = 1, 2, \ldots, n$$

$$c_i(0) = c_{i_0}$$

In the case of the kinetic mechanism we have adopted, given by equations B-2, n is equal to four when the five steady state equations are substituted in the right hand sides. These rate equations take the form:

$$\frac{dc_{NO}}{dt} = f_{NO}\,(c_{NO},\ c_{NO_2},\ c_{HC},\ c_{O_3}) \qquad \text{(B-3a)}$$

$$\frac{dc_{NO_2}}{dt} = f_{NO}\,(c_{NO},\ c_{NO_2},\ c_{HC},\ c_{O_3}) \qquad \text{(B-3b)}$$

$$\frac{dc_{HC}}{dt} = f_{HC}\,(c_{NO},\ c_{NO_2},\ c_{HC},\ c_{O_3}) \qquad \text{(B-3c)}$$

$$\frac{dc_{O_3}}{dt} = f_{O_3}\,(c_{NO},\ c_{NO_2},\ c_{HC},\ c_{O_3}) \qquad \text{(B-3d)}$$

Since the four f_i are nonlinear, equations B-3 must be integrated numerically, usually on a digital computer.

There are a large number of techniques available for the numerical solution of coupled, first-order, ordinary differential equations. Selection of an appropriate technique depends to a large extent on the nature of the system that is represented by the differential equations. Chemically reacting systems, for example, often consist of individual reaction steps having widely disparate time constants (or characteristic reaction times). This is particularly true when fast free radical reactions and much slower initiation and termination reactions are occurring simultaneously. Mathematically, when such a situation exists, the associated system of ordinary differential equations is characterized by eigenvalues* which vary greatly in magnitude. Such a system of equations, termed a "stiff" system,** often presents substantial difficulties in the selection of a numerical integration technique.

To illustrate the problems associated with the integration of stiff differential equations, we consider the linear ordinary equations,

$$\frac{dc_1}{dt} = a_{11}c_1 + a_{12}c_2 \quad ; \quad c_1(0) = 2 \qquad \text{(B-4a)}$$

$$\frac{dc_2}{dt} = a_{21}c_1 + a_{22}c_2 \quad ; \quad c_2(0) = 1 \qquad \text{(B-4b)}$$

---

*The eigenvalues λ_i, $i = 1, 2, \ldots, n$, of a system of ordinary differential equations are those of the n x n Jacobian matrix, J, the element i,j of which is

$$\frac{\partial f_i}{\partial c_j} \qquad i,j = 1, 2, \ldots, n,$$

and are the n solutions of the equation,

$$|J-\lambda I| = 0.$$

**By analogy to the equations describing the oscillations of a mechanical system with a stiff spring.

where

$$A = \begin{bmatrix} a_{11} & a_{12} \\ a_{21} & a_{22} \end{bmatrix} = \begin{bmatrix} -500.5 & 499.5 \\ 499.5 & -500.5 \end{bmatrix}$$

The solution of these equations is

$$c_1 = 1.5e^{-t} + 0.5\ e^{-1000t}$$

$$c_2 = 1.5e^{-t} - 0.5\ e^{-1000t}$$

where the eigenvalues of A are $\lambda_1 = -1000$ and $\lambda_2 = -1$. Both c_1 and c_2 have a rapidly decaying component, corresponding to λ_1, which very quickly becomes insignificant. After a brief initial phase of the solution in which the λ_1 component is not negligible, we would like to proceed, if we were integrating the equations numerically, with a step length Δt which is determined only by the λ_2 solution component.

The conditions for stability of most numerical integration procedures take the form

$$|\lambda_i\ \Delta t| \leq \alpha$$

$$i = 1,2, \ldots, n$$

where α is of the order 1 to 10. If, for example, we wished to use the fourth order Runge-Kutta method (for which $\alpha = 2.785$) for the solution of equations B-4, a necessary condition for ensuring stability is

$$|1000\Delta t| \leq 2.785$$

The maximum allowable Δt, therefore, is 2.785×10^{-3}, which corresponds to nearly 2000 integration steps for a five-second time interval. Thus, although the component of the solution associated with $\lambda_1 = -1000$ disappears early in the integration, we are constrained to use an unacceptably small time step to preserve stability, with the result that computation time is far too large.

A number of techniques for integrating stiff systems of ordinary differential equations have recently been proposed, and these methods are summarized by Lapidus and Seinfeld (1971). The objective of each is to permit the use of a time step that is sufficiently large to ensure economical integration times, while simultaneously maintaining stability. One of the most recent, and most promising, of these methods has been proposed by Gear (1969, 1971). The basic procedure is of the predictor-corrector type, in which one proceeds from the value of c(t) at $t = (n-1)h$ (where $h = \Delta t$) to the value at $t = nh$ by computing a first approximation of c_n

$$c_n^{(0)} = c_{n-1} + h\beta_1 c'_{n-1} + \ldots + h\beta_p c'_{n-p}$$

where p = number of prior values of concentration used to compute c_n,

then iteratively correcting $c_n^{(0)}$ by applying for formula

$$c_n^{(m+1)} = c_{n-1} + h\beta_0^* f(c_n^{(m)}, t_n) + h\beta_1^* y'_{n-1} + \ldots + h\beta_{p-1}^* y'_{n-p+1}$$

for $m = 0, 1, 2, \ldots$ until the computed sequence converges.

(The notation c_n corresponds to $c(t_n)$, with $t_n = nh$. $c_n^{(0)}$ is termed the *predicted* value of c, $c_n^{(m+1)}$ the *corrected* value.) The β_i and β_i^*, which vary for different methods, also assume various values depending on the order of the method used, the order being equal to the number of terms included in the Taylor series approximation of the function $c(t)$ at any point t_n. It is thus necessary that values of these parameters be taken from tables.

Gear's method is based on this predictor-corrector format. The coefficients β_i and β_i^* are chosen so that values of h can be used which are compatible with the non-stiff components of the solution, i.e., those associated with the smaller eigenvalues. The computer program we employed to integrate the reaction rate equations is a slightly modified version of that reported by Gear (1971). Both step size h and order are selected automatically, with the order chosen so as to maximize step size while maintaining stability. The method and program have proven extremely efficient for the solutions attempted thus far, a typical computing time being about three seconds for a 3½ hour smog chamber simulation, using an IBM 360/75 computer.

V. VALIDATION OF THE NEW SIMPLIFIED MECHANISM

Having considered the selection of reaction rate constants and stoichiometric coefficients and the problems encountered in the numerical integration of the coupled ordinary differential equations, we turn now to validation of the kinetic mechanism. Validation was undertaken for four hydrocarbon systems:

	Reactant	Data Source
1	propylene	Gulf Research Corp. (Strickler (1970)) State of California Air Resources Board (Wayne, et al. (1970))
2	isobutylene	Aerospace Corporation and Stanford Research Institute (Westberg, et al. (1971))
3	n-butane	Battelle (Wilson (1971))
4	propylene/n-butane mixture	Battelle (Wilson (1971))

The selection of each hydrocarbon (or mixture of hydrocarbons) served a particular purpose. In the case of propylene, data were available for two initial HC:NO_x ratios; ability to represent smog chamber data for various HC:NO_x ratios is an important attribute of a mechanism. The isobutylene data were valuable, as the experiments in which they were obtained were carried out both in the presence and absence of CO; the capability of the model to represent the effects of CO could thus be studied. While both propylene and isobutylene are olefins and are thus characteristic of highly reactive hydrocarbons, n-butane, the third hydrocarbon studied, is a less reactive species. It was thus of interest to determine if the mechanism could approximate the concentration/time behavior of smog chamber experiments for this paraffin. Finally, the study of mixed hydrocarbon systems is a critical step in achieving adequate representation of the reaction characteristics of the highly complex mixture of hydrocarbons found in the atmosphere. We were fortunate to obtain data for the propylene/n-butane system, a mixture of two hydrocarbons having widely differing reactivities. In this section, we present validation results for each of the four hydrocarbon systems and conclude with a discussion of the effect of initial NO_x concentrations on ozone formation.

Propylene

The major objective of this study was to evaluate the ability of the mechanism to predict concentration/time behavior for different initial ratios of hydrocarbon to nitrogen oxides. Initial conditions and selected values of stoichiometric coefficients and rate constants for the validation are given in Table B-6.* Predicted concentrations and experimental data are shown in Figures B-6 and B-7.

The comparison between prediction and experiment for the two validation runs are, in general, favorable. Experimentally measured NO_2 peaks occur at 75 minutes and 85 minutes as compared with predicted peaks of 68 minutes and 103 minutes respectively. While there are significant differences between prediction and experiment for NO_2, propylene, and ozone at various instances in time, similar trends are apparent.

In the case of propylene, α was taken to be

$$\alpha = \begin{cases} 2.45 & [NO]/[HC] < 0.25 \\ 9.8 \dfrac{[NO]}{[HC]} & 0.25 < [NO]/[HC] < 1 \end{cases}, \qquad \text{(B-5)}$$

as this relationship (1) provided validation of the two propylene experiments with all other parameters fixed, and (2) demonstrated the correct dependence of peak ozone concentrations on initial NO:HC ratio for ratios from 1/4 to 1 (See data of Altshuller, et al. (1967)). For $[NO]/[HC] < 0.25$, $\alpha = 2.45$ insures that a minimum number of free radicals are generated, even when the NO concentration is low. Although we did not have validation data for the range $[NO]/[HC] > 1$, we would expect α to decrease with an increase in the ratio, as peak ozone concentrations decrease over this range. The values of 2.45 and 9.8 have no significance other than the fact that they give good validation for the experiments shown.

*In the presentation of validation results for each of the four hydrocarbon systems, only the values of rate constants that differ from base values are given in Table B-6. See Table B-4 for values of the remaining constants.

Figures B-6 and B-7 and Table B-6 follow.

TABLE B-6. Parameters and Initial Reactant Concentrations Used in Validation of the New, Simplified Mechanism

Hydrocarbon	Propylene		Isobutylene		n-Butane		Propylene/ n-Butane
	Strickler (1970)	Wayne, et al. (1970)	Westberg, et al. (1971)	Westberg, et al. (1971)	Wilson (1971)	Wilson (1971)	Wilson (1971)
For validation results, see Figure	B-6	B-7	B-8	B-9	B-10	B-11	B-12
Initial Concentrations							
$[HC]_o$ ppm	3.29	1.0	3.0	3.0	3.05	3.05	0.56/3.4
$[NO]_o$ ppm	1.612	1.0	1.5	1.5	0.49	0.50	0.48
$[NO_2]_o$ ppm	0.088	0.1	0.04	0.04	0.106	0.106	0.098
$[CO]_o$ ppm	0	0	0	100	0	100	0
$[HC]_o / [NO_x]_o$	1.95	0.91	1.95	1.95	5.1	5.1	6.8
Stoichiometric Coefficients							
α	see eq. (B-5)		see eq. (B-5)		5.0		3.0
β	1.7		1.9		0.5		0.67
δ	0.8		0.2		1.2		1.2
θ	0.02		0.22		0.61		0.53

(continued on next page)

TABLE B-6 (continued)

Hydrocarbon	Propylene		Isobutylene		n-Butane		Propylene/ n-Butane
	Strickler (1970)	Wayne, et al. (1970)	Westberg, et al. (1971)	Westberg, et al. (1971)	Wilson (1971)	Wilson (1971)	Wilson (1971)
For validation results, see Figure	B-6	B-7	B-8	B-9	B-10	B-11	B-12
Reaction Rate Constants**							
k_1*	0.37		0.355		0.40		0.40
k_6	0.037		0.0355		0.04		0.04
k_9	5.0×10^4		3.1×10^4		2.0×10^3		see eq. (B-6)
k_{10}	0.0075		0.017		0.001		see eq. (B-6)
k_{11}	1.0×10^3		1.0×10^4		6.0×10^3		see eq. (B-6)
k_{4a}	.006						
k_{4bc} †	.1						
k_5	.0025						
k_{12}	1800		Same for all validation runs				
k_{13}	10						
k_{14}	1800						

*Photolysis rate, as reported by experimenter.

**The unit of k_1 and k_6 are min^{-1}, all other rate constants, ppm^{-1} min^{-1}.

† Rate constant for reactions 4b and 4c combined.

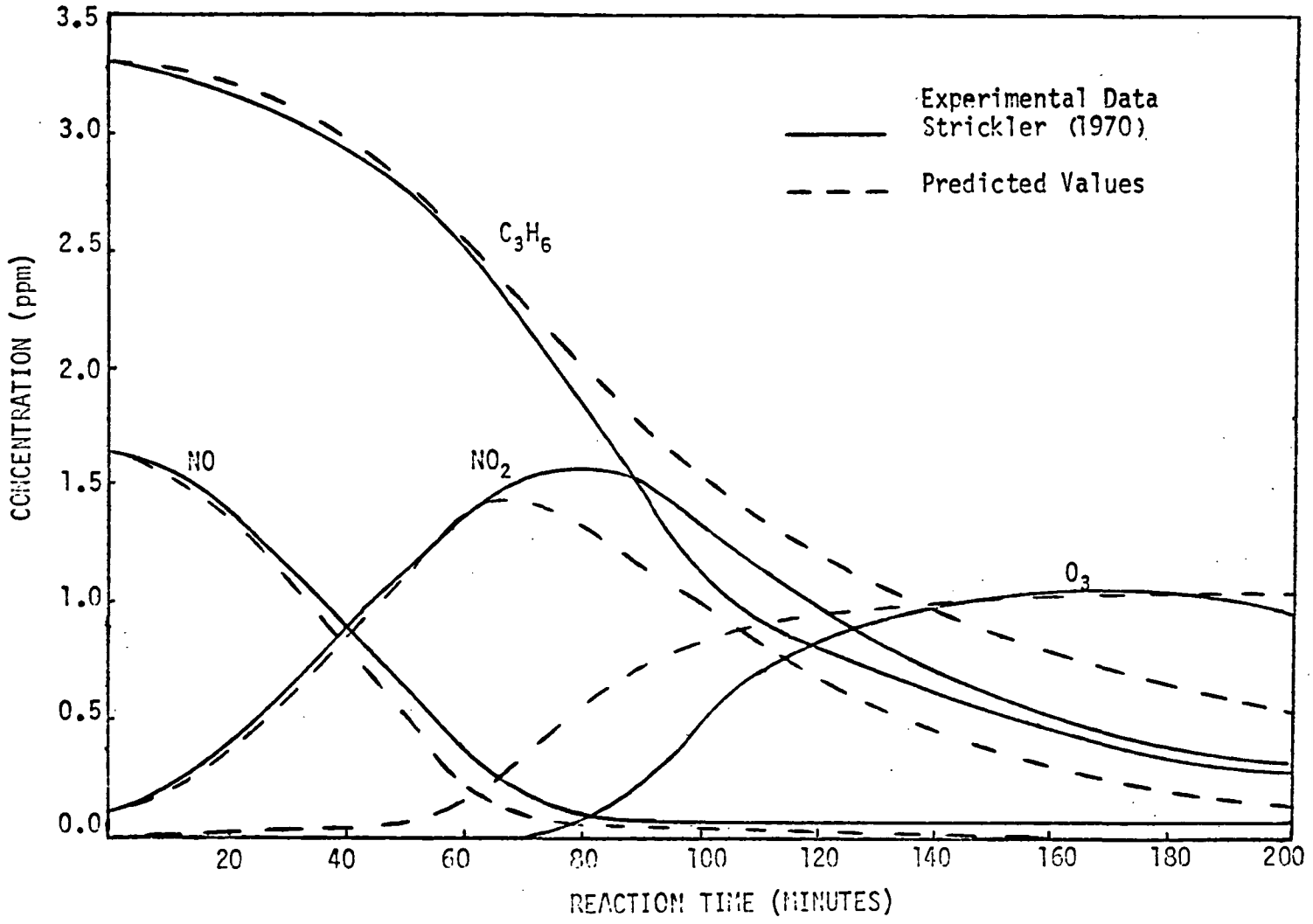

FIGURE B-6. VALIDATION OF THE NEW MECHANISM - PROPYLENE

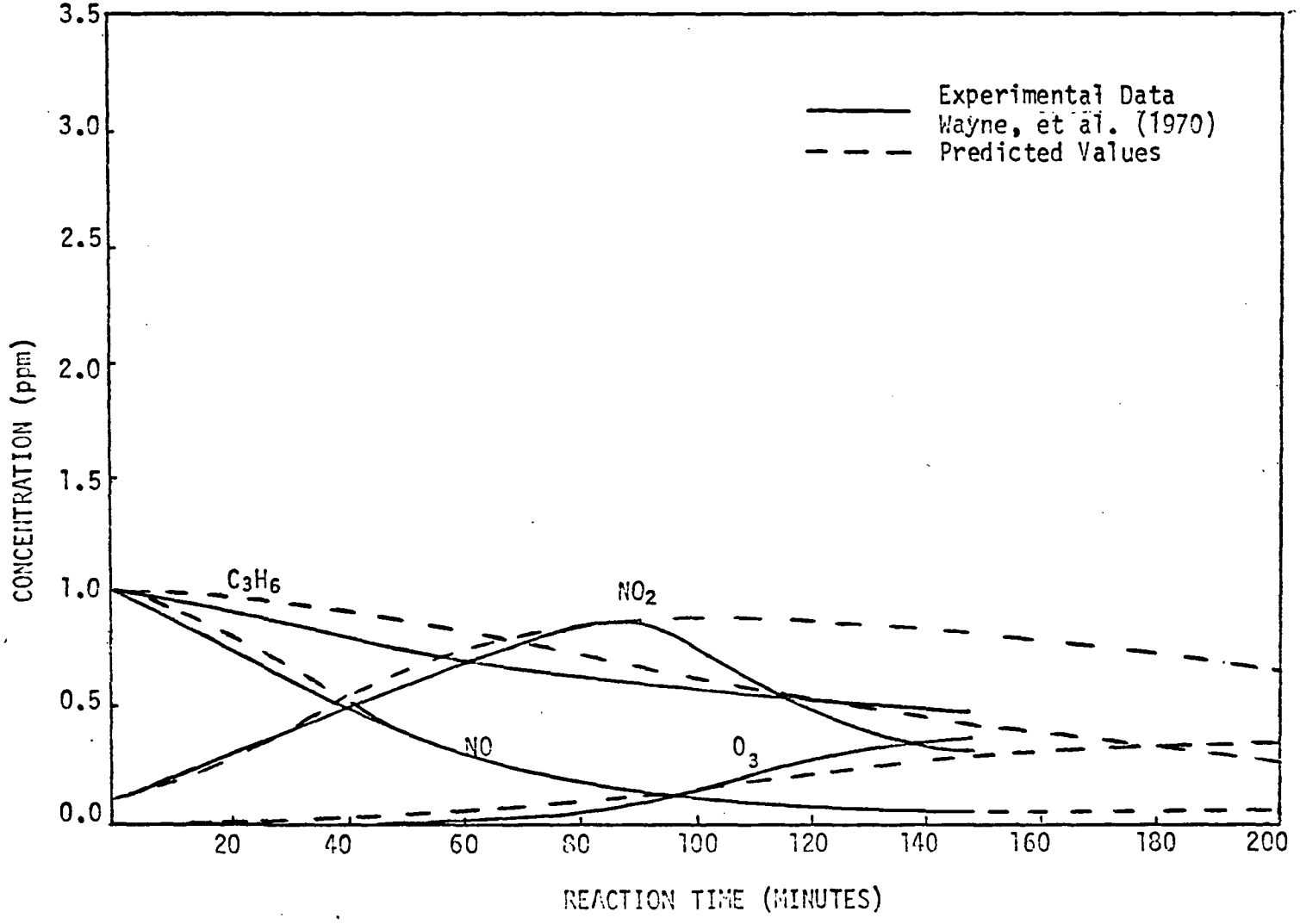

FIGURE B-7. VALIDATION OF THE NEW MECHANISM - PROPYLENE

Isobutylene

The objectives of this portion of the study were to examine the ability of the model to represent the effect of CO on reaction rates and to evaluate the mechanism using a second olefin. See Table B-6 for initial conditions and values of selected parameters, Figures B-8 and B-9 for validation results and experimental data.

Comparison of prediction and experiment are quite good for both of the isobutylene experiments, at zero and 100 ppm carbon monoxide. In particular, the model predicts earlier peaking of NO_2 (by 32 minutes, in accord with experiment), accelerated accumulation of O_3, and more rapid oxidation of the olefin in the presence of CO than in its absence. The only significant deviation between prediction and experiment is that which occurs for isobutylene after 100 minutes in the absence of CO. Finally, note that α was treated in the same manner as in the propylene validation.

n-Butane

The purpose of this portion of the study was to investigate the ability of the mechanism to describe the reaction dynamics of a species less reactive than the two olefins studied thus far, with alterations being made in only the hydrocarbon rate constants and the stoichiometric coefficients. The values of these parameters are given in Table B-6, the validation results in Figures B-10 and B-11. It should be noted that the simulations in these figures are for six hours, nearly double that for the previous olefin simulations. Comparisons between prediction and experiment are excellent.

A few comments may be helpful regarding the treatment of three parameters in this validation. First, in contrast to the variable α used in the propylene and isobutylene studies, a constant value of this parameter was employed for n-butane because of its low reactivity relative to olefins. Secondly, non-zero values of both k_{10} and β were used even though ozone does not react with n-butane to any appreciable degree. This is necessary because olefins probably are some of the first stable products to appear as a result of the reaction of O and $OH\cdot$ with n-butane, and their formation must be accounted for. A possible reaction scheme for the generation of olefins is

$$C_4H_{10} + O \longrightarrow C_4H_9\cdot + OH\cdot$$

$$C_4H_{10} + OH\cdot \longrightarrow C_4H_9\cdot + H_2O$$

$$CH_3CH_2CH_2CH_2\cdot \longrightarrow C_2H_5\cdot + CH_2 = CH_2$$

$$CH_3CH_2\dot{C}HCH_3 + O_2 \longrightarrow (CH_3)_2C = CH_2 + HO_2\cdot$$

The formation of isobutylene in the butane oxidation may be evidenced by the fact that several products observed in the butane photo-oxidation for example, acetone and PAN (Altshuller (1969))--are the same as those found in isobutylene photo-oxidation.

Figures B-8 to B-11 follow

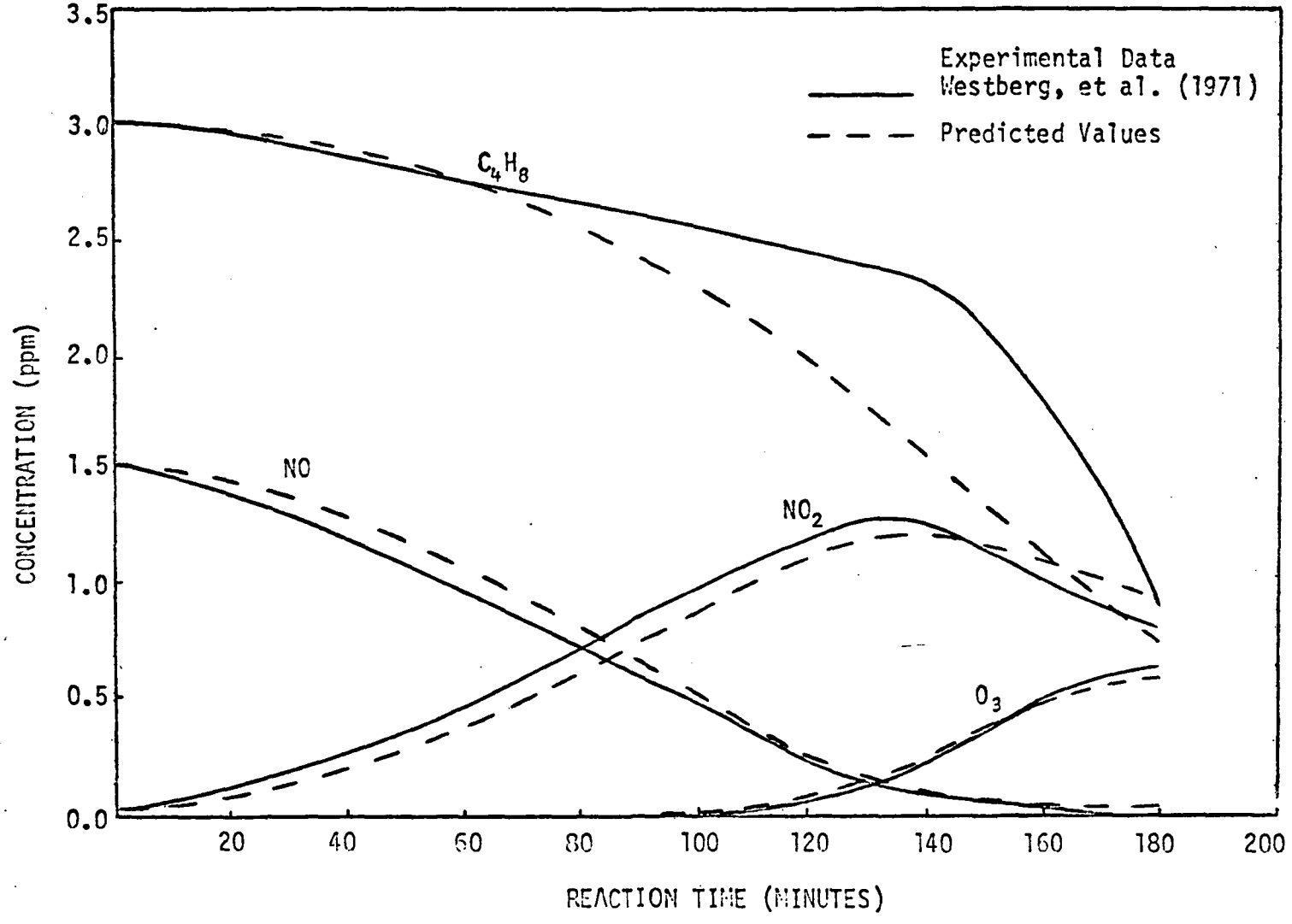

FIGURE B-8. VALIDATION OF THE NEW MECHANISM - ISOBUTYLENE (NO CARBON MONOXIDE)

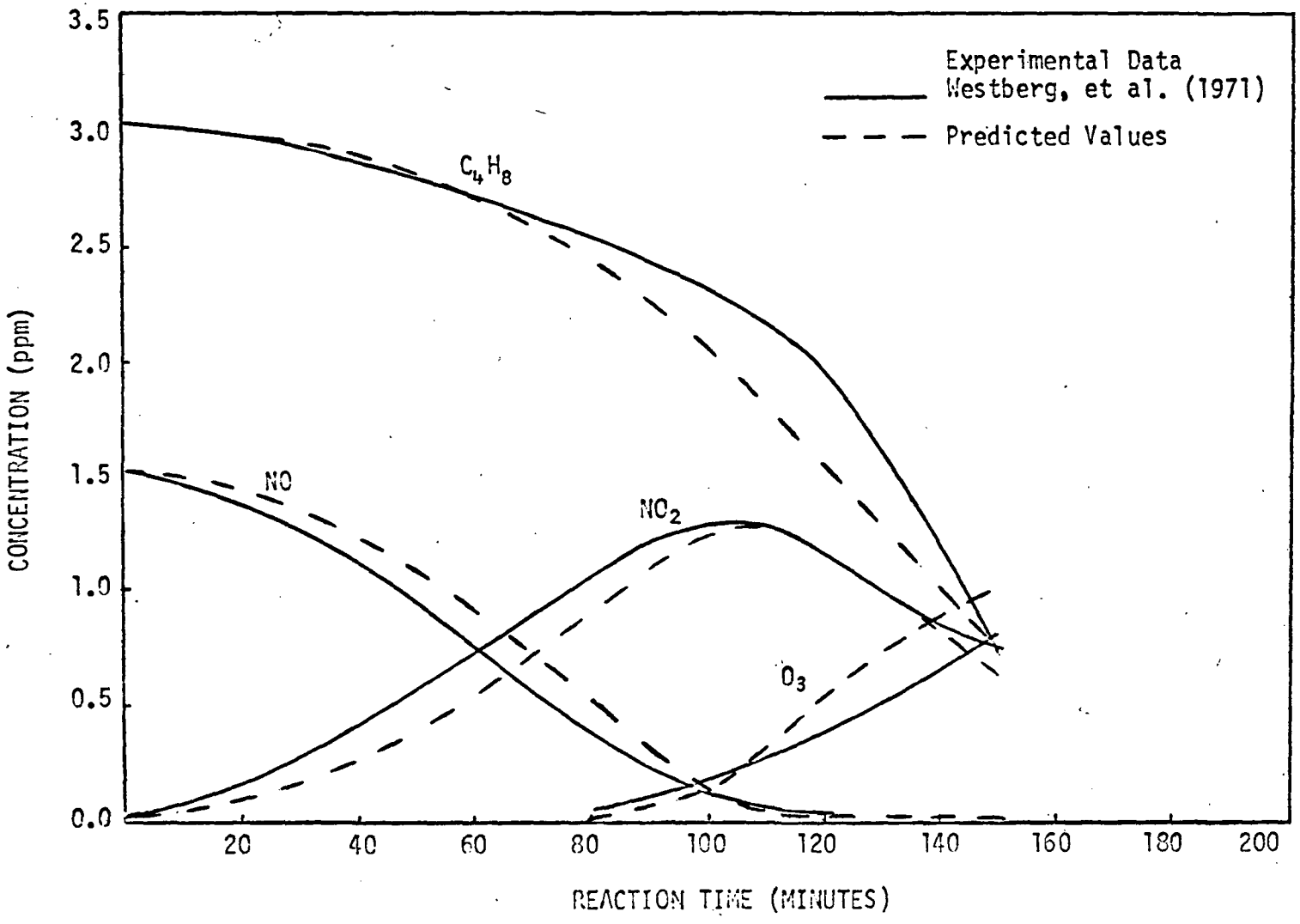

FIGURE B-9. VALIDATION OF THE NEW MECHANISM - ISOBUTYLENE (100 ppm CARBON MONOXIDE)

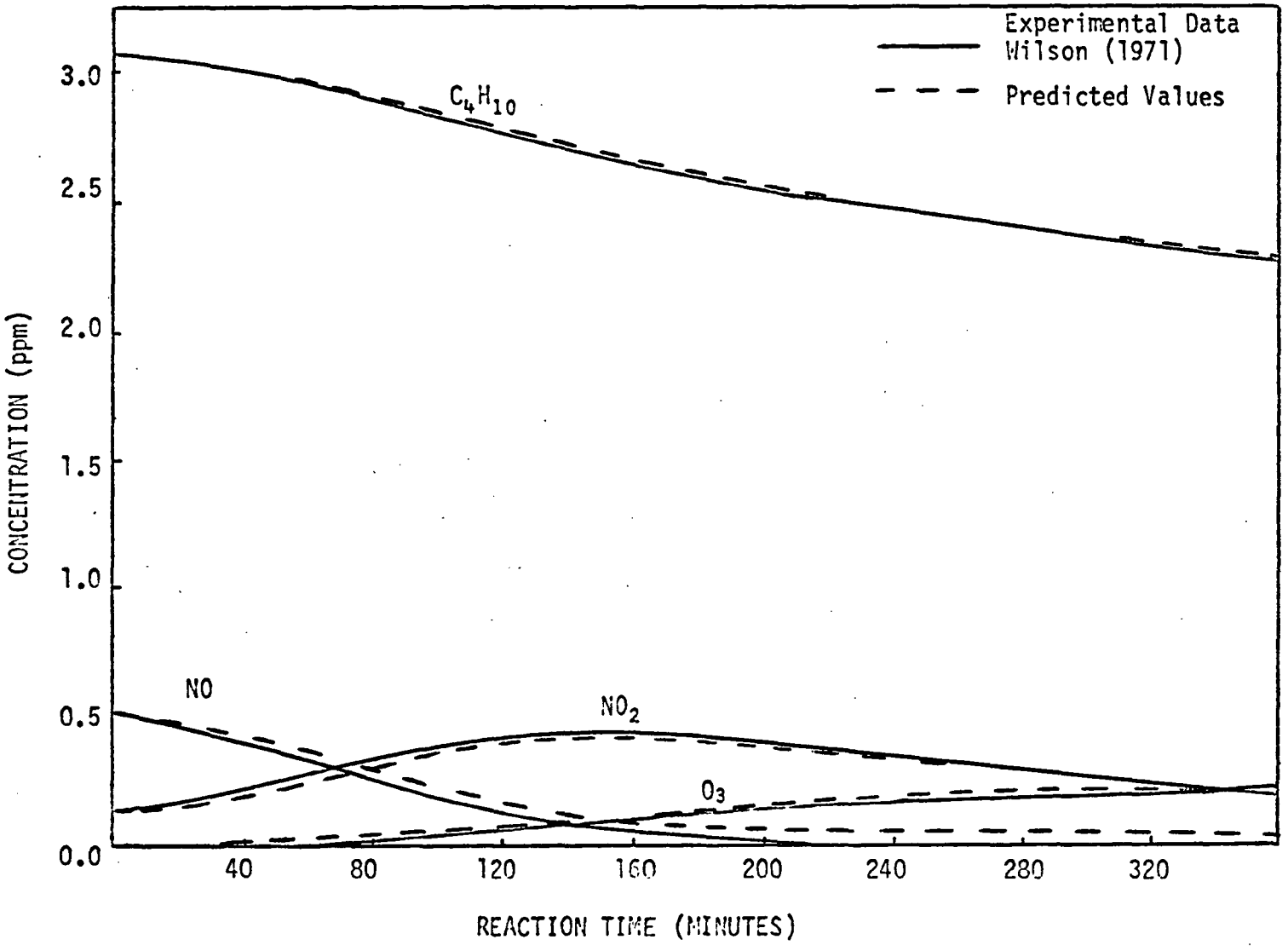

FIGURE B-10. VALIDATION OF THE NEW MECHANISM - N-BUTANE (NO CARBON MONOXIDE)

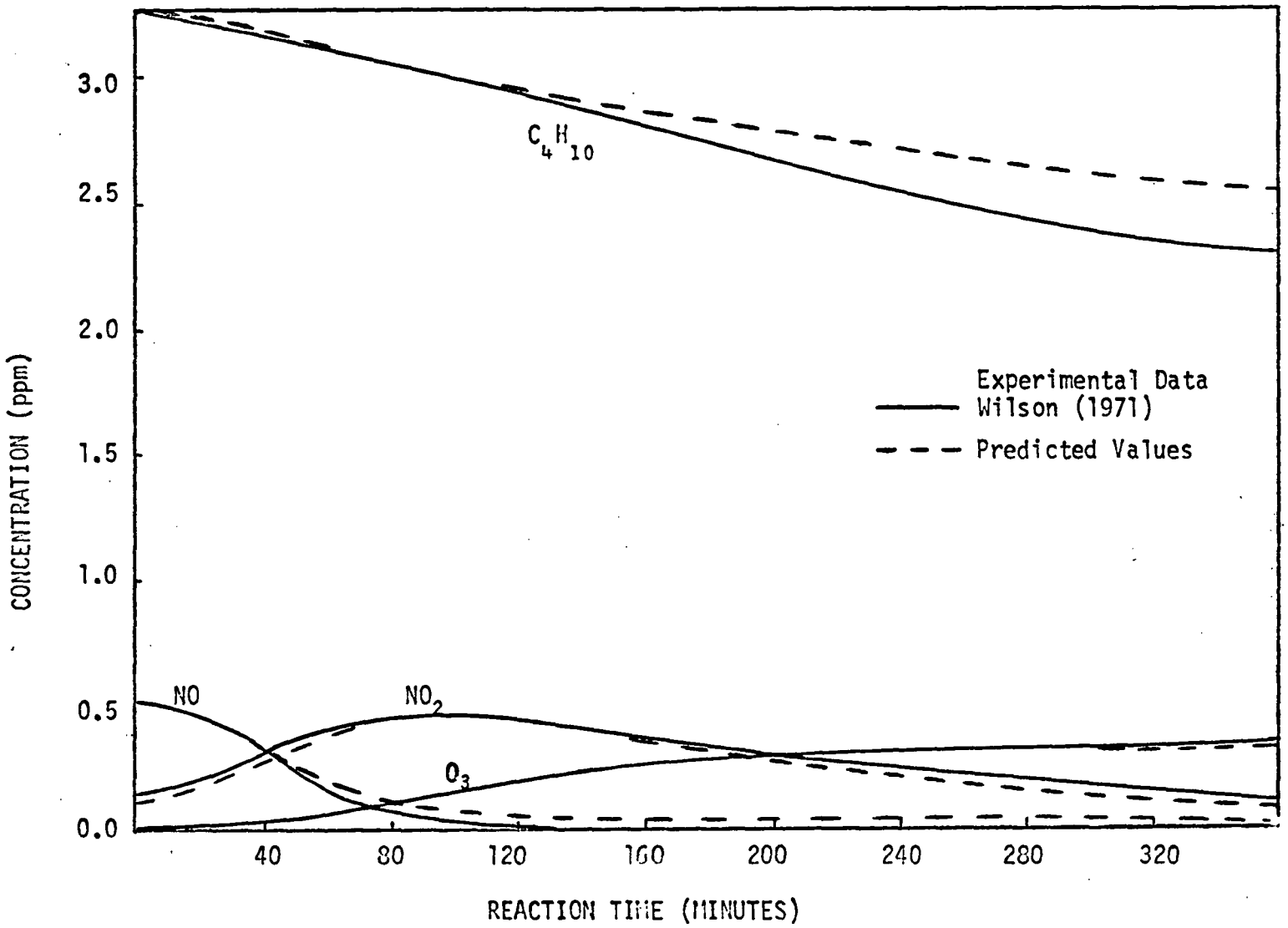

FIGURE B-11. VALIDATION OF THE NEW MECHANISM - N-BUTANE (100 ppm CARBON MONOXIDE)

Propylene and n-Butane

We now consider the photo-oxidation of a mixture of propylene and n-butane, carried out experimentally by Wilson (1971). The purpose of this portion of the validation effort was to explore the possibility of deriving rate constants and stoichiometric coefficients for the mixture from values established previously for the pure hydrocarbons species. As a first step, both types of parameters were calculated for the mixture of propylene and n-butane as linear combinations of values established for the pure components, weighted in proportions to the fraction of each in the initial mixture. Thus,

$$k_{i_{mixture}} = f\, k_{i_p} + (1-f)\, k_{i_b} \qquad \text{(B-6)}$$

where k_{i_p} = rate constant for reaction i for propylene

k_{i_b} = rate constant for reaction i for n-butane

f = fraction of propylene in the initial reaction mixture

This method of deriving rate constants for hydrocarbon mixtures is similar in nature to the "combined rate" approach used by Glasson and Tuesday (1971).

In initial validation runs, we found that the combined rate approach predicted a greater oxidation rate than was observed experimentally, a phenomenon also reported by Glasson and Tuesday. However, by altering the value of k_{13} from the combined rate value of 96 to a new value of 45, we obtained the results shown in Figure B-12. Aside from this one alteration, all parameters were computed using equation B-6 and values of pure hydrocarbons shown in Table B-6. (Note that α is again treated as a constant). As can be seen in Figure B-12, adoption of the "combined rate" method results in close agreement between prediction and experiment. However, much more study of this approach is needed.

NO_x Inhibition

Extensive experimental evidence indicates that, after a certain point, an increase in the initial concentration of NO_x will result in a decrease in the maximum concentration of ozone observed (Glasson and Tuesday (1970)). One of the key requirements that a simplified mechanism must satisfy is that it demonstrate this inhibitory effect of NO_x on peak ozone concentration. In this closing section, we explore the capability of the new mechanism to satisfy this requirement. Before presenting the results of this study, however, we wish to comment on the type of data needed in order to investigate this effect adequately.

Figure B-12 follows.

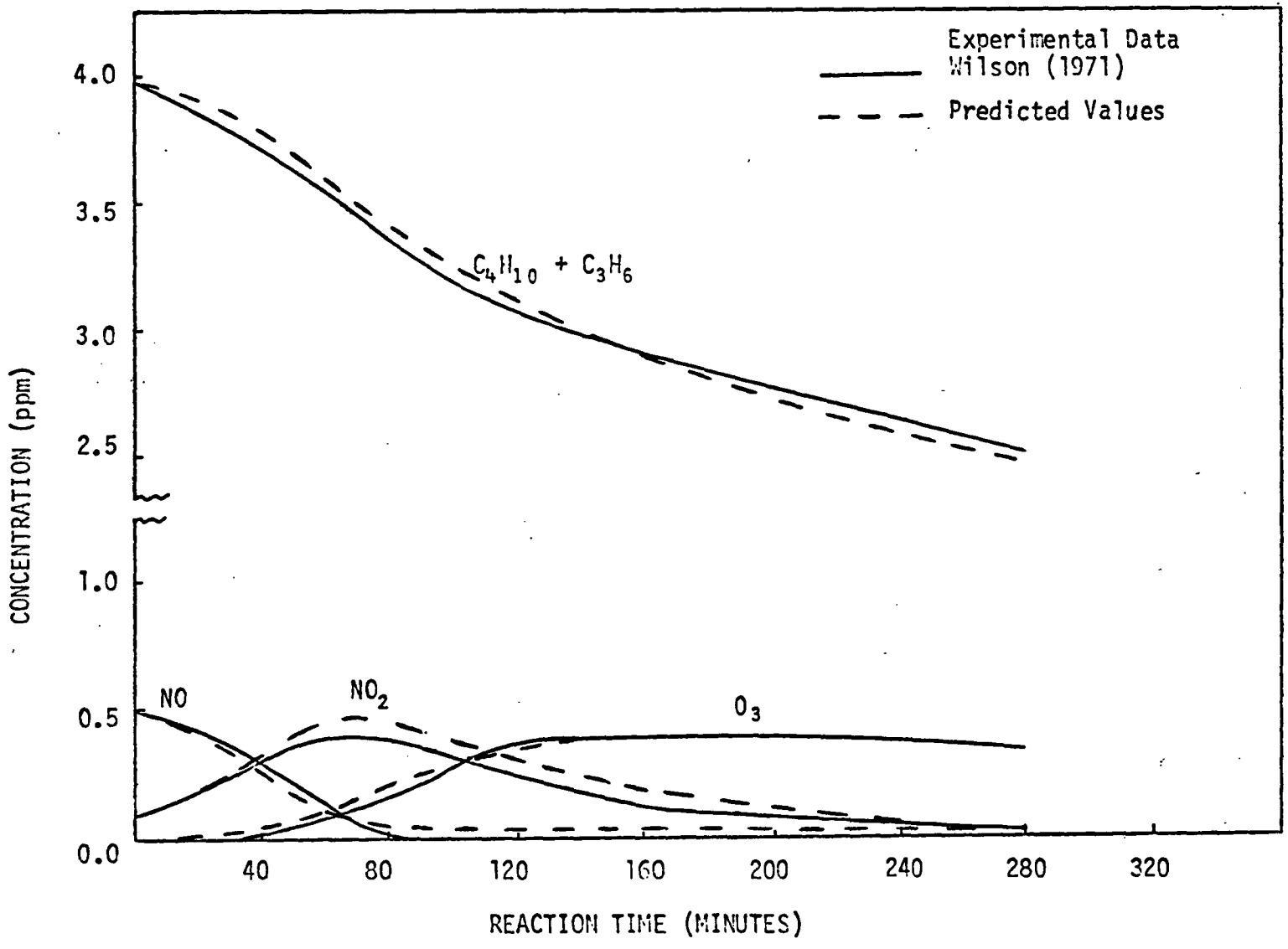

FIGURE B-12. VALIDATION OF THE NEW MECHANISM - PROPYLENE/N-BUTANE

It is not unusual that the results of smog chamber experiments be presented in the form of ozone concentration after a fixed time of irradiation (say two hours) as a function of (or plotted against) initial concentration of NO_x at a fixed initial hydrocarbon concentration. However, information of this type is useless because the time to the NO_2 peak and the time at which O_3 appears are dependent on the individual concentrations of NO and NO_2, not only on the NO_x concentration. Individual NO and NO_2 concentrations must also be reported. To demonstrate this point, we carried out two simulations, in each of which $[HC]_o:[NO_x]_o = 2:1.1$. In the first case, the NO_x was composed of 0.1 ppm NO_2 and 1.0 ppm NO, in the second, 0.4 ppm NO_2 and 0.7 ppm NO. In the first case NO_2 peaked at 94 minutes, in the second, at 57 minutes. Although the concentration of ozone ultimately reached about the same maximum level in both cases, after two hours the two concentrations were 0.424 and 0.634 ppm, respectively. The peak ozone formation rate, defined and and reported by Glasson and Tuesday (1970) as $[O_3]_{max}/2t_{\frac{1}{2}}$, where $t_{\frac{1}{2}}$ is the time required for the attainment of one-half the peak ozone concentration, is also highly dependent on the composition of NO and NO_2 in the initial reaction mixture. These points are illustrated in Table B-7, in which the simulated results of three runs are reported. In each run the initial concentration of NO_x was 1.1 ppm, but the initial NO concentration was varied. It is clear from these results that if smog chamber data are reported in terms of either $[O_3]_{2\ hrs.}$ or $[O_3]_{max}/2t_{\frac{1}{2}}$, *both* the initial NO and NO_2 concentrations must be reported.

Having warned the reader about the use of data in which nitrogen oxides are lumped together, we proceed to use such data anyhow, largely because the desired type of data were unavailable. Altshuller, et al. (1967) have reported results pertaining to oxidant concentration as a function of $[NO_x]_o$ at fixed $[C_3H_6]_o$. Even though the individual $[NO]_o$ and $[NO_2]_o$ were not reported, the irradiation time for each run was six hours, insuring that the peak O_3 level had been reached. Their results are shown by the solid curve in Figure B-13. Note a sharp inhibition at initial NO_x concentrations greater than about 2.5 ppm for experiments involving initial propylene concentrations of 2 ppm. We have simulated these runs using the new simplified mechanism with $[NO_2]_o = 0.1$ ppm. The results are shown by the dashed curve in Figure B-12. It is important to realize that NO inhibition is reflected in the model by the choice of α, so that Figure B-13 demonstrates only that the choice of α is consistent with observed behavior.

VI. ADAPTATION OF THE NEW MECHANISM FOR INCORPORATION INTO AN URBAN AIRSHED MODEL

We have to this point focused our attention on the development and validation of a kinetic mechanism capable of describing atmospheric photochemical reactions. As has been noted, validation refers to the comparison between predictions of the mechanism and experimental results

Table B-7 and Figure B-13 follow

TABLE B-7. Effect of Initial NO and NO_2 Concentrations on the Time of Appearance of O_3

$[C_3H_6]_o$ = 2 ppm, $[NO_x]_o$ = 1.1 ppm

$[NO_2]_o$ ppm	$[NO]_o$ ppm	$[O_3]_{max}$ ppm	$t_{½}$, min	$[O_3]_{2\ hrs}$ ppm	$[O_3]_{max}/2t_{½}$
0.05	1.05	0.734	127	0.311	2.89×10^{-3}
0.10	1.00	0.741	113	0.424	3.28×10^{-3}
0.40	0.70	0.789	77	0.634	5.12×10^{-3}

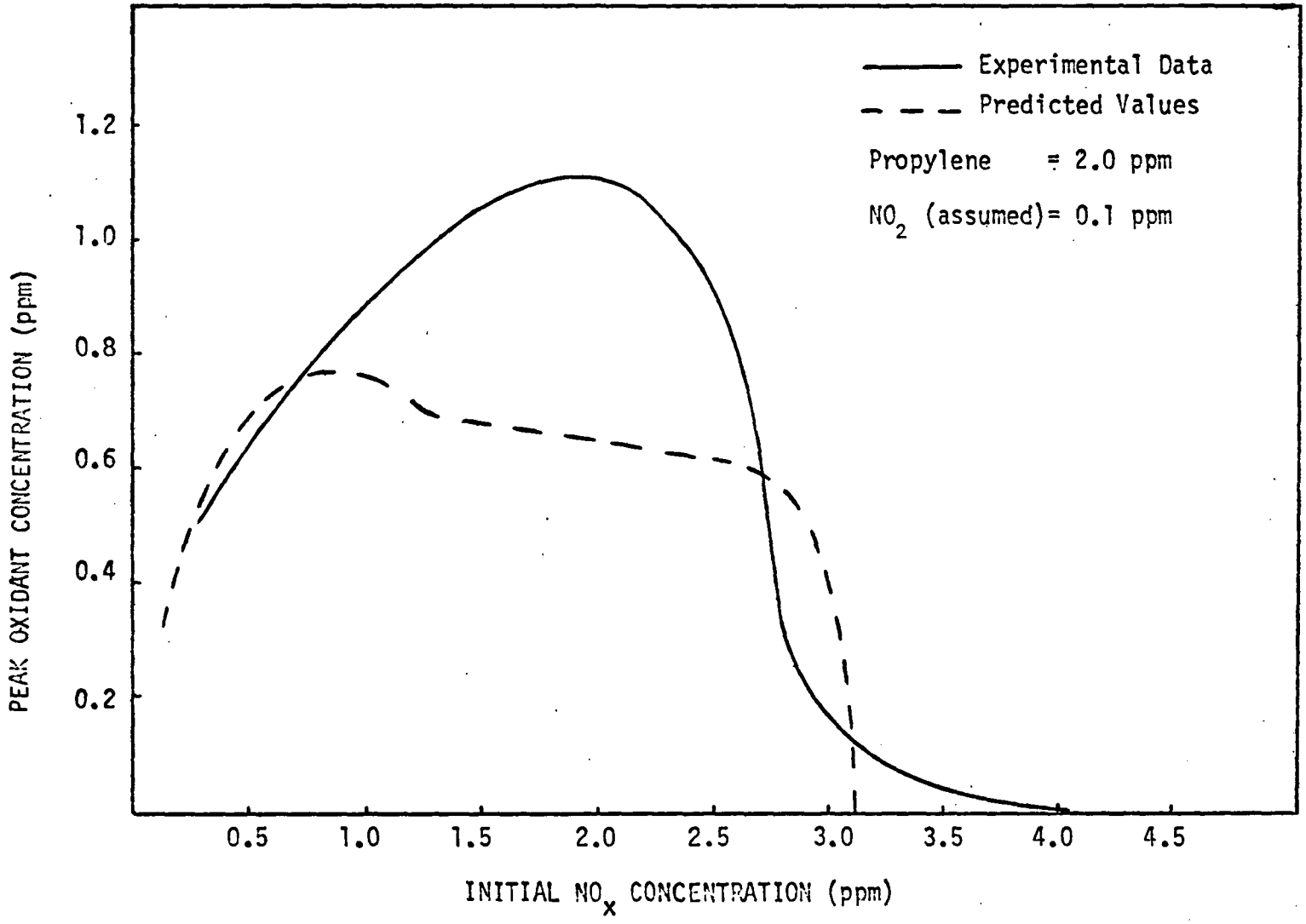

FIGURE B-13. RELATIONSHIP BETWEEN INITIAL NO_x CONCENTRATION AND PEAK OXIDANT CONCENTRATION

based on smog chamber studies. However, smog chamber experiments are not directly representative of atmospheric reaction conditions. Specifically, such experiments are commonly carried out at constant intensity of radiation (and fixed spectral distribution) and for hydrocarbon reactants consisting of a single species, a simple mixture, or a complex mixture "representative" of atmospheric contaminants. Before we can incorporate the new, simplified mechanism into an urban airshed model, it is necessary to account for temporal variations in intensity of incoming radiation and for variations in the reaction rate of the generalized hydrocarbon species, HC, and its associated free radical, $RO_2^{\cdot}$, due to overall changes in the composition of the mixture of hydrocarbons in the atmosphere.

A. The Effects of Solar Radiation on Rates of Photolysis

The sun, the sky, and the surface of the earth are all sources of the radiation that is received by the lower atmosphere. The quantity (or intensity) of radiation received is dependent on the magnitude and spectral distribution of the radiant flux density outside the atmosphere, the amount of scattering, absorption, and reflection by the atmosphere, the albedo of the earth's surface, and the solar zenith angle. The amount of radiation absorbed by a particular species is primarily a function of the spectral distribution and the intensity of incoming radiation, but is also a function of concentration and specific physical and electronic properties of the species in question. Of particular interest to us is the influence of incoming solar radiation on the rates of decomposition (or photolysis) of NO_2 and HNO_2, the two species considered in the mechanism upon which solar radiation has a significant effect.

Accounting properly for the effects of these many variables on the intensity and distribution of incoming solar radiation is an extremely complex undertaking. We have incorporated some of the variables into our treatment, and not others. In particular, the effect of zenith angle on radiation intensity is included by relating the reaction rate constants, k_1 (for NO_2) and k_6 (for HNO_2), to latitude, time of the year, and time of day. We have not attempted to deal with the effects of cloud cover, as days on which high concentrations of photochemical pollutants occur are days of virtually cloudless skies over the Los Angeles Basin. In addition, we have not accounted for the effect on k_1 and k_6 of variations in aerosol concentration (due to absorption and scattering) either as a function of time or as a function of elevation above the ground. We believe that considerably more must be known about the scattering and diffusion of radiant energy due to the presence of aerosols before these effects be properly incorporated into our model, and that, in any case, our current level of knowledge of atmospheric reactions is insufficient to merit the inclusion of such detailed phenomena.*

* See Leighton (1961, Ch. 2) for a discussion of the nature of solar radiation and its absorption in the polluted layer of the atmosphere.

We have accounted for variations in k_1 and k_6 rather simply. First, consider k_1. Leighton (1961) presents a plot, reproduced in Figure B-14, of $(k_1/\phi k_3)$* as a function of time (PST) for both summer and winter solstice conditions in Los Angeles. This plot is applicable to the latitude of Los Angeles and may be used as the basis for representing variations in k_1 with time of year and time of day for cloudless days and for atmospheres relatively free of particulates. To derive this relationship:

(1) We interpolated between the summer and winter solstice curves in Figure B-14 to obtain a curve representative of our validation period, late September. This is the dashed line in the figure.

(2) Using values of k_3 from Johnston and Crosby (and given on page 154 of Leighton) that are based on estimates of temperature as a function of time for the validation days of 29 and 30 September 1969, we calculated (k_1/ϕ) as a function of time (see Table B-8).

(3) We normalized k_1/ϕ by dividing it by the largest hourly value achieved during the day, which occurs at 11 a.m. The normalized variable f ranges from zero to one.

(4) Finally, our estimated relationship between k_1 and time for the late September validation period is derived by multiplying f by 0.37 minutes^{-1}, the value of k_1 that is typical of conditions of maximum intensity.

The derived curve is shown in Figure B-15 and is given by the quadratic equation,

$$f = 1.017 - .068\tau - 1.076\tau^2 \qquad \text{(B-7)}$$

where $\tau = \frac{t - 12}{6}$

t = time in hours (PST)

and $0 \leq t \leq 24$

(Note: This equation represents a fit to the curve in Figure B-15, and is applicable only to the two validation days stated, since a specific temporal distribution of temperature is assumed. However, we will generalize this relationship in future work to include ambient temperature and time of year as independent variables.)

The photolysis of HNO_2 has not been investigated as thoroughly as has the photolysis of NO_2. In the absence of more pertinent data, we have assumed that the temporal variation of k_6 is the same as that of k_1, given by Equation B-7. Thus, $k_6 = (k_6)_{max} f$, for the validation days, 29 and 30 September, 1969, where $(k_6)_{max}$ is taken to be $0.1(k_1)_{max}$ or .037 min^{-1}. (Johnston, et al. (1970)).

---

*ϕ is the fraction of photolytically excited NO_2 molecules which actually react.

Figures B-14 and B-15 and Table B-8 follow.

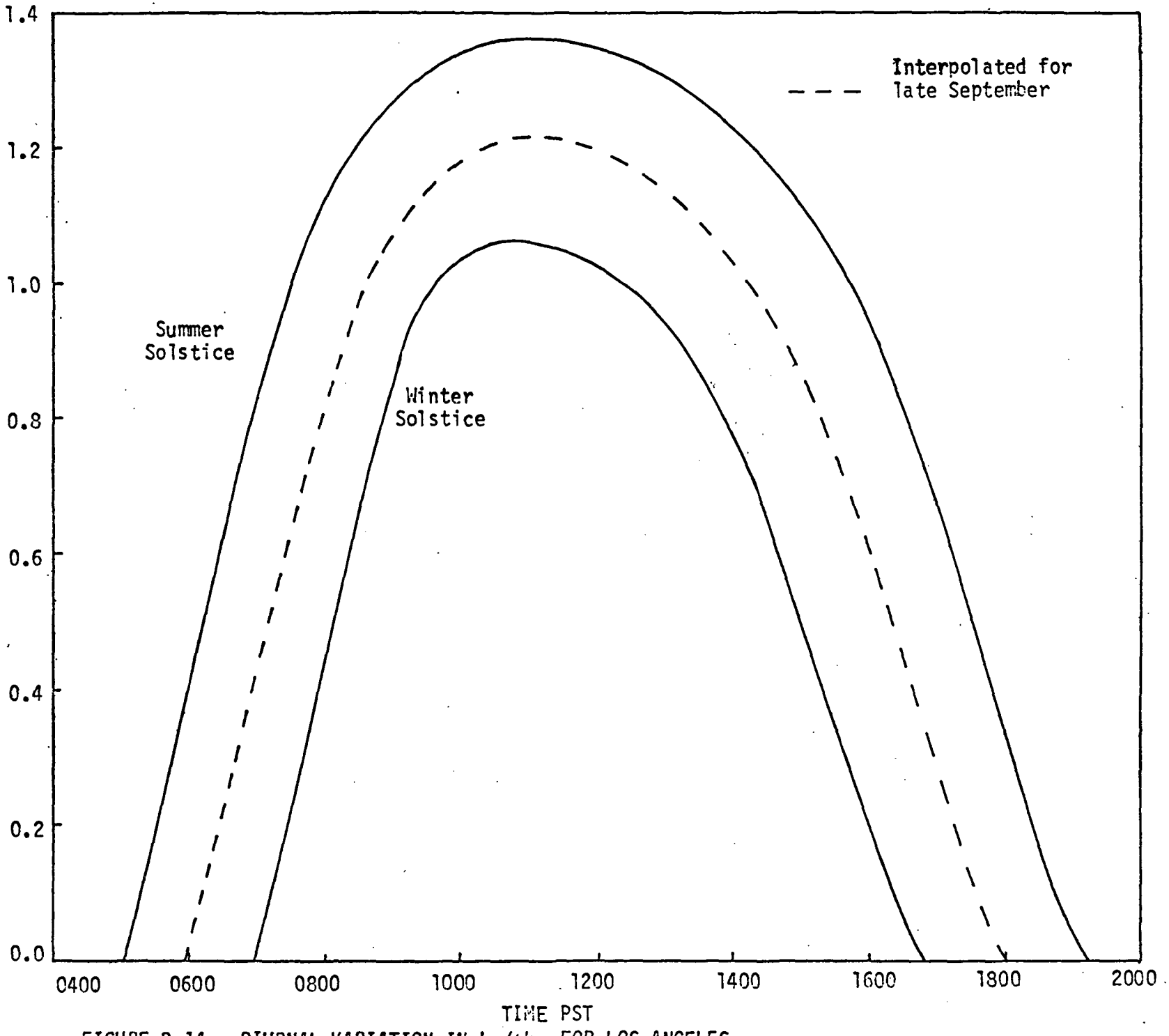

FIGURE B-14. DIURNAL VARIATION IN $k_1/\phi k_3$ FOR LOS ANGELES

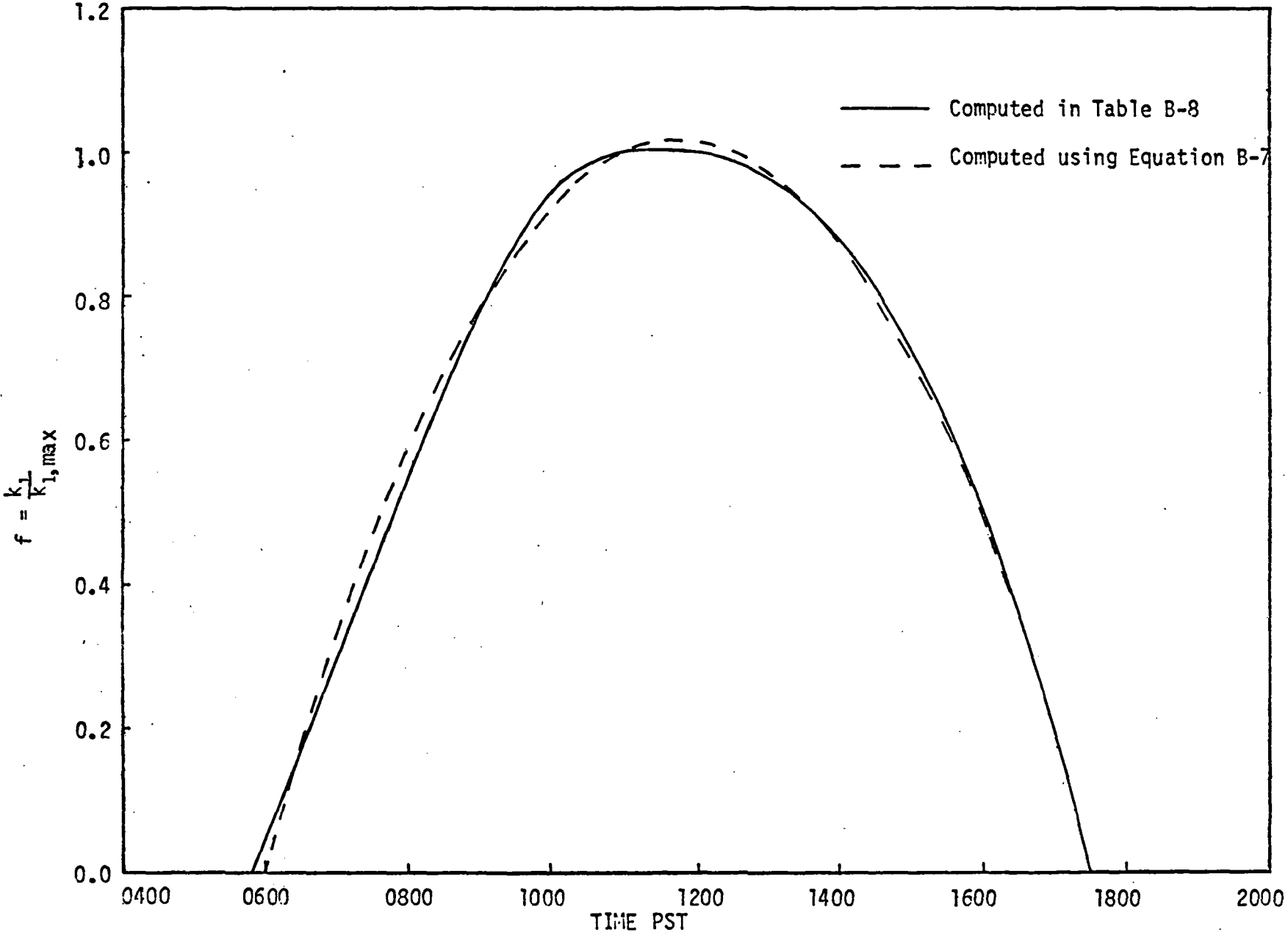

FIGURE B-15. DIURNAL VARIATION IN f FOR LOS ANGELES FOR 29 and 30 SEPTEMBER 1969

TABLE B-8. Determination of f and k_1 as a Function of Time of Day for 29 and 30 September 1969

Time of day (PST)	$\frac{k_1}{\phi k_3}$ (pphm) *	Estimated** Temperature (°F)	k_3 (pphm^{-1}hr^{-1}) †	k_1/ϕ (hr^{-1})	f $\left(= \frac{k_1}{k_{1,max}}\right)$ ††	k_1 (min^{-1})
6 AM	.06	62	15.3	.918	.041	.015
7	.43	66	15.7	6.751	.301	.111
8	.76	70	16.2	12.312	.549	.203
9	1.02	78	17.4	17.748	.791	.293
10	1.16	85	18.3	21.228	.946	.35
11	1.20	88	18.7	22.440	1.000	.37
Noon	1.18	90	19.0	22.420	.999	.37
1 PM	1.15	90	19.0	21.850	.974	.36
2	1.05	90	19.0	19.950	.889	.33
3	.86	90	19.0	16.340	.728	.27
4	.59	86	18.4	10.856	.484	.18
5	.26	82	17.8	4.628	.206	.076
6	zero	75	16.9	zero	zero	zero

* Taken from the dashed curve in Figure B-14.

** Estimated average hourly temperatures for the days 29 and 30 September 1969.

† Interpolated values, taken from k_3 vs. temperature given by Johnston and Crosby (see Table 44, p. 154, Leighton (1961)).

†† See Figure B-15 for a plot of the function.

B. Variations in Reactivity of Atmospheric Hydrocarbons.

We have demonstrated in Section V that the new, simplified mechanism is capable of simulating the important features of hydrocarbon photo-oxidation reactions observed in the laboratory. However, as has been pointed out, it is not clear that the smog chamber and the atmosphere are equivalent reaction systems. By incorporating the validated mechanism into the overall airshed, we are in effect assuming that phenomena characteristic of smog chamber experiments, such as NO_x inhibition and CO acceleration, are also characteristic of atmospheric reactions. This assumption is a fundamental premise in the formulation and development of the airshed model.

We will employ *two* lumped hydrocarbons, an *unreactive* species HC_u and a *reactive* species HC_r, in the overall airshed model. The unreactive species will include only those hydrocarbons which do not undergo appreciable reaction during the course of a day. Individual hydrocarbons are classified as reactive or unreactive according to the hydrocarbon reactivity scale of Bonamassa and Wong-Woo (1966), shown in Table B-9. We have chosen to include in the category HC_u only those hydrocarbons, with the exception of propane, having zero reactivity on this scale. Propane is treated as reactive, since the rate constant for the propane/OH· reaction is much closer to that of butane than that of ethane. Thus, the lumped hydrocarbon HC_u will consist of ethane, benzene, acetylene, and methylacetylene and will be treated as an inert substance in the simulation. The species HC_r represents the reactive mixture, composed of all other hydrocarbons, and is identical to the species HC in the new, simplified mechanism.

While the assignment of individual hydrocarbons to specific reactivity groups is unambiguous, a consistent procedure has not yet been developed for the estimation of rate constants and stoichiometric coefficients for reactions occurring in the atmosphere. There are a number of reasons for this. The density of pollutant emissions vary over space and time. The more reactive species (those in reactivity classes 5 through 9) may be consumed with sufficient rapidity that the composition of the hydrocarbon mixture in the atmosphere, and thus its reactivity, declines during the course of the day. (However, Eschenroeder and Martinez (1970), in analyses of Los Angeles contaminant data collected at two sites, were unable to detect variations in reactivity). Furthermore, even though we have assumed that the behavior of a mixture of hydrocarbons may be similar to the average behavior of the individual species (see Section V, validation of the propylene/n-butane system), the generality of this assumption has not been established. Finally, by virtue of our inclusion of a generalized hydrocarbon in the mechanism, it is not possible to distinguish in the simulation among the various reactive species that constitute HC_r.

---

*Methane is present in the atmosphere in large quantities relative to other hydrocarbons. As it derives predominantly from natural sources, is inert, and is a ubiquitous atmospheric constituent, it will not be included in HC_u or treated in the model.

Table B-9 follows.

TABLE B-9. Scale of Relative Reactivities for Hydrocarbons*

Reactivity**	Representative Hydrocarbon Species
0	methane, ethane, propane, acetylene, methylacetylene, benzene
1	butanes and higher paraffins, cycloalkanes
3	toluene
4	ethylene
5	ethylbenzene, m- and p-xylene
6	o-xylene, tri- and tetramethylbenzenes, propadiene
7	1-alkenes
8	2-alkenes

* Proposed by Bonamassa and Wong Woo (1966)

** Based on product yield and biological effects when hydrocarbons are irradiated in the presence of oxides of nitrogen.

As of this writing, we plan to pursue the following course. We will select constant values of reaction rate constants and stoichiometric coefficients (except for α) so as to obtain the best overall prediction during the course of the day. Values of certain parameters--notably k_9, k_{10}, k_{11}, α, β, and δ--will likely be modified from values established in smog chamber studies (and reported in Table B-6) during initial validation, in order to account for characteristics of the atmospheric system that are at variance with those observed in the laboratory. Should this approach prove inadequate, we will investigate the possibility of dividing HC_r into two or more categories to represent more precisely the reactivity of the atmospheric hydrocarbon mixture. This approach may also be an aid in detecting spatial and temporal variations in reactivity, as Eschenroeder and Martinez considered only the average reactivity of a single lumped species in their study.

REFERENCES

Altshuller, A. P., Bufalini, J. J., Photochem. Photobiol., 4, 97 (1965).

Altshuller, A. P., Kopszynski, S.L., Lonneman, W. A., Becker T.L., Slater, R., Environ. Sci. Technol., 1, 899 (1967).

Altshuller, A. P., Jour. Air Pollution Control Assoc., 19, 787 (1969).

Altshuller, A. P., Bufalini, J. J., Environ. Sci. Technol., 5, 39 (1971).

Baulch, D. L., Drysdale, D. D., Lloyd, A. C., High Temperature Reaction Rate Data - No. 1, The University, Leeds, England (1968).

Behar, J.,"Simulation Model of Air Pollution Photochemistry," Project Clean Air, Univ. of California, Volume 4 (Sept. 1, 1970).

Bonamassa, F., Wong-Woo, H., "Composition and Reactivity of Exhaust Hydrocarbons From 1966 California Cars," presented before the Division of Water, Air and Waste Chemistry 152nd National Meeting American Chemical Society, New York, N.Y. (September 11-16, 1966).

Clyne, M. A. A., Thrush, B. A., Wayne, R. P., Trans. Faraday Soc., 60, 359 (1964).

Eschenroeder, A. Q., "Validation of Simplified Kinetics for Photochemical Smog Modeling," IMR-1096, General Research Corp., Santa Barbara, Calif. (Sept. 1969).

Eschenroeder, A. Q., Martinez, J. R., "Analysis of Los Angeles Atmospheric Reaction Data From 1968 and 1969," CR-1-170, General Research Corporation, Santa Barbara, Calif. (July 1970).

Eventova, M. S., Prytkova, G. N., Vestnik Moskov Univ. Ser. II, 5, 59 (1960).

Ford, H. W., Doyle, G. J., Endow, N., J. Chem. Phys., 26, 1337 (1957).

Friedlander, S. K., Seinfeld, J. H., Environ. Sci. Technol., 3, 1175 (1969).

Gear, C. W.,"The Automatic Integration of Stiff Ordinary Differential " Equations, Information Processing 68,(A. J. H. Morrell, Editor) North Holland Publ. Co., Amsterdam, pp. 187-193 (1969).

Gear, C. W., "The Automatic Integration of Ordinary Differential Equations," Communications of the ACM, 14, 3, 176-190 (1971).

Glasson, W. A., Tuesday, C. S., Environ. Sci. Tech., 4, 1, 37 (1970).

Glasson, W. A., Tuesday, C. S., Environ. Sci. Technol., 5, 151 (1971).

Greiner, N. R., J. Chem. Phys., 53, 1070 (1970).

Hecht, T. A., Seinfeld, J. H., "Development and Validation of a Generalized Mechanism for Photochem. Smog," Environ. Sci. Tech., submitted for publication (1971).

Holmes, J. R., "Atmospheric Photochemistry - Some Factors Affecting the Conversion of NO to NO_2," Sixth Western Regional Meeting Amer. Chem. Soc., Pacific Conf. on Chem. and Spectroscopy, San Francisco (Oct. 6-9, 1970).

Johnston, H. S., Pitts, J. N., Jr., Lewis, J., Zafonte, L., Mothershead, T., "Atmospheric Chemistry and Physics," Project Clean Air, Volume 4, University of California (Sept. 1, 1970).

Kaufman, F., Kelso, J. R., J. Chem. Phys., 46, 4541 (1967).

Kemula, W., Grobowska, A., Bull. Acad. Polon. Sci., Ser. Sci. Chim., 8, 525 (1960).

Lapidus, L. and J. H. Seinfeld, Numerical Solution of Ordinary Differential Equations, Academic Press, New York (1971).

Leighton, P. A., Photochemistry of Air Pollution, Academic Press, New York (1961).

Schott, G., Davidson, N., J. Amer. Chem. Soc., 80, 1841 (1958).

Stedman, D. H., Morris, E. D., Jr., Daby, E. E., Niki, H., Weinstock, B., "The Role of OH Radicals in Photochemical Smog Reactions," 160th National Meeting Amer. Chem. Soc., Chicago (Sept. 13-18, 1970).

Stephens, E. R., Air Water Pollut. Int. J., 10, 649 (1966).

Strickler, P. D., private communication (1970).

Wayne, L. G., Danchick, R., Weisburd, M., Kokin, A., Stein, A., "Modeling Photochemical Smog on a Computer for Decision Making," Sixth Western Regional Meeting Amer. Chem. Soc., Pacific Conf. on Chemistry and Spectroscopy, San Francisco (Oct. 6-9, 1970).

Wayne, L. G., Earnest, T. E., "Photochemical Smog, Simulated by Computer," 62nd Annual Meeting Air Poll. Cont. Assoc., paper 69-15, New York (June 1969).

Wayne, L. G., Yost, D. M., J. Chem. Phys., 19, 41 (1951).

Westberg, K., Cohen, N., "The Chemical Kinetics of Photochemical Smog as Analyzed by Computer," ATR-70 (8107)-1, The Aerospace Corp., El Segundo, Calif. (Dec. 1969).

Westberg, K., Cohen, N., Wilson, K. W., Science, 171, 1013 (1971).

Wilson, W. E., private communication (1971).

Zafonte, L., Rate Constants for Atmospheric Reactions, Project Clean Air, Volume 4, Univ. of California (Sept. 1, 1970).